ABSTRACT

A STUDY OF NUCLEAR ENERGY LEVELS IN ^{121}Sb, ^{123}Sb, ^{125}Sb AND ^{127}I USING β- AND γ-RAY SPECTROSCOPY

by Ronald L. Auble

The decay schemes of several odd-A tellurium (A = 121, 127) and tin (A = 123, 125) isotopes have been examined in an effort to gain information about the nuclear level structure of adjacent antimony and iodine isotopes. Beta- and gamma-ray singles and coincidence spectroscopy were used to determine the ordering of the gamma-ray transitions, and therefore, the energies of the nuclear levels. Several levels which had been unobserved in earlier studies were located in each of the four isotopes. Angular correlation measurements on the prominent gamma-gamma cascades in ^{121}Sb, ^{125}Sb and ^{127}I were made to study the spins of the nuclear states and the mixing ratios of the gamma-ray transitions. The spectrum shape of the beta-rays feeding one of the excited states in ^{123}Sb was studied and found to yield an essentially linear Fermi-Kurie plot. This result, in conjunction with the corresponding log ft value, suggests a non-unique, first forbidden assignment for this beta transition and limits the possible spin assignments for the ^{123}Sb state.

Comparisons are made of the existing experimental data with the predictions of several nuclear models: In the low energy regions of ^{121}Sb and ^{127}I, sufficient data on mixing ratios and lifetimes are available to make quantitative comparisons with predictions of the single particle model and with the

pairing-plus-quadrupole residual interaction calculations of Kisslinger and Sorensen. Partial agreement is found between the experimental data and the latter predictions.

At higher excitations, only qualitative comparisons can be made due to the lack of gamma-ray lifetime and mixing ratio measurements. A model which is found to predict level structure similar to that observed experimentally is one in which the low-lying particle states are coupled to excitations of the nuclear core. However, several high energy states in ^{125}Sb are found to deviate from the predictions of this model. Thus, other types of excitation must also be assumed to exist. The nature of these states can only be determined after additional experimental data become available.

A STUDY OF NUCLEAR ENERGY LEVELS IN ^{121}Sb, ^{123}Sb, ^{125}Sb AND ^{127}I USING β- AND γ-RAY SPECTROSCOPY

By

Ronald L. Auble

A THESIS

Submitted to
Michigan State University
in partial fulfillment of the requirements
for the degree of

DOCTOR OF PHILOSOPHY

Department of Physics and Astronomy

1966

ACKNOWLEDGEMENTS

I wish to express my deepest appreciation to Dr. William H. Kelly for his aid and guidance during the experimental work and the preparation of this thesis. I thank Dr. Herbert H. Bolotin for suggesting this region of the isotope table for study and for his aid in understanding the theory and application of angular correlations.

Mr. G. Berzins, Mr. L. Beyer, Mr. R. Etherton and Mr. D. Gollnick aided in the acquisition and analysis of experimental data.

I acknowledge the financial assistance of the National Science Foundation which provided partial support for the experimental program. During much of the time in which this program was in progress, I was supported by a Fellowship from the Michigan Institute of Science and Technology.

Last, but definitely not least, I thank my wife Shirley for her continued moral support and encouragement.

TABLE OF CONTENTS

LIST OF TABLES

LIST OF FIGURES

INTRODUCTION

Among the more interesting nuclei to be studied both experimentally and theoretically in recent years, are those having odd-A and spherical equilibrium shapes.[1,2,3] The spherical shape is deduced from the properties of the ground states of these nuclei, especially their small electric quadrupole moments. Of particular interest are those isotopes which have a single nucleon outside a closed shell. The ground states and, in most cases, the first few excited states of such nuclei, have been studied experimentally and the spins and parities, where known, are in reasonable agreement with Single Particle Model predictions. Many of these states, however, have no spin assignments. Even less is known about the higher energy states (> 600 keV) of these nuclei and it is obvious that additional data will have to be obtained before any comparisons can be made with theoretical predictions. This is especially true for the antimony isotopes which have 51 protons.

In order to study the excited states of these isotopes, it is necessary to populate them by means of the radioactive decay of adjacent isobars. This requires that the parent nucleus have a reasonably long half life (> 1 day). The antimony isotopes ^{121}Sb, ^{123}Sb and ^{125}Sb meet this requirement and are therefore well suited for this study. (The isotope ^{119}Sb is populated by long-lived ^{119}Te. However, the parent nuclide could not be produced by the methods available to us at the time.) In addition to the antimony nuclei, which differ from each other by the addition

of pairs of neutrons, it is of interest to examine a nucleus having an added pair of protons. Thus, the levels in ^{127}I are studied. This particular isotope is chosen since the known low energy level structure appears similar to that of ^{121}Sb and it meets the requirement of having a long-lived parent.

The experimental methods employed in these studies are those of beta and gamma ray spectroscopy. The introduction of more sophisticated electronic instrumentation and the development of new detectors in recent years has greatly increased the value of these techniques. Two particularly important advances have been the introduction of multichannel-multiparameter analyzers for accumulation of large quantities of coincidence data in a minimum of time, and the development of high resolution semiconductor gamma-ray detectors. The use of these new developments, as well as more conventional instruments and methods, in these investigations, makes possible more accurate and complete descriptions of the nuclear level structure of the isotopes under study than were previously possible.

CHAPTER 1

NUCLEAR MODELS

Since one of the objectives of experimental studies, such as these, is to compare experimental data with theoretical predictions, a brief outline of several nuclear models and some of their predictions will be presented.

1.A. The Nuclear Shell Model

As already pointed out, the low lying states of many odd mass nuclei are described, at least in part, by the Single Particle Model.[4,5] In this model, which is the simplest form of the nuclear Shell Model,[4,6] the nucleons are considered to move independently of each other in an average static potential, for example, a harmonic oscillator potential. In order to reproduce the experimental "magic numbers" (deduced from binding energies, magnetic moments, etc.)[4] it was necessary to include in the Hamiltonian a spin orbit term, that is, a term proportional to $\underline{s}\cdot\underline{l}$, which splits the levels having $j = \ell + \frac{1}{2}$ and $j = \ell - \frac{1}{2}$. The sign of this interaction is found empirically to be negative since the states having $j = \ell + \frac{1}{2}$ lie below those with $j = \ell - \frac{1}{2}$. The result is a set of levels described by the quantum numbers (nlj). For the nuclei being studied here, which have both N and Z between 50 and 82, the single particle states available are the $(2d_{5/2})$, $(1g_{7/2})$, $(2d_{3/2})$, $(3s_{1/2})$ and $(1h_{11/2})$. This is the order suggested by Mayer and Jensen[4] for an unpaired proton. The excited states of the nucleus, in this model, are assumed to be

due to the promotion of the unpaired nucleon to the higher energy single particle states.

As may be expected, such a simple model cannot, and indeed does not, explain the more detailed properties of nuclei, even in those isotopes near closed shells. The classic examples usually given are the E2 transition rates and electric quadrupole moments in certain nuclei.[7] These are almost invariably larger than the single particle estimates, often by several orders of magnitude. One model which has been employed in attempting to account for these effects is the "Extended" Shell Model (or Intermediate Coupling Shell Model). The first attempts to extend the range of validity of shell model calculations consisted in the removal of the requirement that the particles move independently by including two-particle interactions. This was first done for particles in a single configuration, namely that giving the lowest energy. This restriction was later removed and "configuration mixing" introduced. This corresponds to using a wave function which is a linear combination of wave functions for single particle states having nearly degenerate energies and the same total angular momentum. The principle difficulty in applying this model was the complexity of the calculations when more than two or three particles are present outside the closed shell. The usefulness of calculations including residual interactions has recently been extended and will be discussed later.

1.B. The Nilsson Model

A second technique which has been applied to explain the

large quadrupole effects in nuclei is the use of spheroidal potentials. In this case, the nucleons are still considered to move independently but the potential well in which they move is no longer spherical. This model has been developed primarily by Nilsson (hence, the Nilsson Model).[8] In the calculation by Nilsson, the particles are assumed to move in a potential given by

$$V_i = V_o\{(1 + \tfrac{2}{3}\delta)(x_i^2 + y_i^2) + (1 - \tfrac{4}{3}\delta)z_i^2\} + C\boldsymbol{\ell}_i \cdot \boldsymbol{s}_i + D\boldsymbol{\ell}_i^2 .$$

The first term is the axially symmetric spheroidal potential, the second is the spin orbit coupling term as used in the single particle model and the third term is introduced, on semi-empirical grounds, to lower the energy of high spin states. The single particle energies are then calculated as a function of δ, the deformation parameter. To apply the model to a given nucleus, one must calculate the equilibrium deformation by minimizing the total energy of the nucleus with respect to δ and then use this deformation parameter, in general different for each state, to deduce nuclear properties. Calculations of equilibrium deformations using the Nilsson Hamiltonian, with slight modifications (principally the inclusion of a pairing force and Coulomb effects) have been made by Marshalek, Person and Sheline,[9] by Bes and Szymanski[10] and by Szymanski.[11] This model has had success at predicting spins, parities and relative level orderings of nuclear states of odd-A deformed nuclei as well as accounting for the large quadrupole effects observed in the deformed regions. (The deformed regions are presently taken to include the nuclei

with $A \sim 25$, $150 < A < 190$ and $A > 224$, and possibly others.)[9]

1.C. The Collective Model: Even-Even Nuclei

Even with the refinements mentioned, many nuclear properties cannot be predicted by shell model calculations. It appears that certain nuclear properties, for example the level structure of many even-even nuclei, can only be explained by the collective motion of the nucleons. This leads to the collective model, introduced earlier by Bohr,[12] in which the nucleus is assumed to undergo two basic motions, rotation and vibration. For even-even nuclei far from closed shells, the observed spin, parity and ordering of the levels are in reasonable agreement with the results obtained from the rotation of an axially symmetric rotator. Such a model is characterized by a series of levels with angular momenta $I = 0, 2, 4, 6, ..$ whose energies are given by

$$E_I = \frac{\hbar^2}{2\mathcal{I}_1} I(I+1)$$

where $\mathcal{I}_1$ is the moment of inertia about the "1" axis (the "3" axis being the symmetry axis).

The energy levels of a non-axially symmetric rotator have been studied by Davydov and Filipov.[13] One major difference between the results for axial and for non-axial symmetry is that the latter shape gives rise to 3^+, 5^+,... states, as well as even spin levels. A relationship which may be applied to test this model is that the sum of the energies of the first two excited 2^+ states should equal the energy of the 3^+ state. There appears to be some evidence that this model may be particularly useful in

the "transition" nuclei between closed shells and regions of large deformation.

The second type of motion to be considered, vibrational, has been introduced to account for certain higher energy states and the levels observed in nuclei between the rotational regions and the closed shells. The nucleus is usually assumed to have a sharp surface whose shape changes with time. The quanta of these shape oscillations are referred to as phonons. In the regions near closed shells, the nucleus is assumed to undergo vibrations about a spherical equilibrium shape, while elsewhere the vibrations will, in general, be about a deformed shape. The resultant level structure in the spherical case, assuming only quadrupole vibrations are present, will be a 2^+ state at energy $\hbar\omega$, a triplet, produced by coupling two phonons, with spins 0^+, 2^+, 4^+ at $2\hbar\omega$, etc. Many spherical even-even nuclei show structure similar to these predictions, although the cases where all three of the 0, 2, 4 triplet states have been observed appear to be quite scarce.

In the deformed regions, vibrations can still take place although the energies are usually much larger than those of rotational levels. In general, the two types of motions will be coupled with the result being the construction of rotational bands on each of the vibrational states, much as in molecular spectroscopy.

I.D. The Collective Model: Odd-A Nuclei

Thus far, we have considered the collective excitations only

in the even-even nuclei. Similar excitations can be expected in the odd mass nuclei as well, requiring the coupling of collective and particle states. In the deformed regions, the coupling will be between single particle states obtained using a deformed well (Nilsson levels in the axial symmetry case) and the rotations of the deformed, either axially symmetric or non-axially symmetric, core. This, the strong coupling limit, has been discussed for the axially symmetric case by Kerman.[14] The energy level spectrum obtained is given by

$$E_{J,K} = \epsilon_K + \frac{\hbar^2}{2\mathcal{J}} [J(J+1) - 2K^2 + \delta_{K,\frac{1}{2}} a(-)^{J+\frac{1}{2}} (J+\tfrac{1}{2})]$$

where ϵ_K = single particle energy; J = total angular momentum; K = projection of J on the symmetry axis; $\mathcal{J}$ = moment of inertia. The decoupling parameter, a, expresses the strength of the coupling between particle and rotational motions. The structure is therefore that of a rotational band built on each of the particle states. This model has been very successful in predicting the levels in odd-A deformed nuclei.

The excited states of odd mass nuclei having non-axially symmetric deformations has been considered only recently by Pashkevich and Sardaryan.[15] The several comparisons with experiment made by these authors are quite good for nuclei in the deformed region: $A = 25$, $150 < A < 190$, and $A > 224$. Calculations were also made for the "spherical" nucleus ^{119}Sb. The experimental data are still very incomplete for all but the first few excited states. However, several of the observed states fit

quite well into the predicted level scheme. Additional spin-parity measurements will need to be made before the applicability of the model to nuclei outside the deformed regions can be ascertained.

At the other extreme of coupling, that is weak coupling, the nucleus consists of a particle coupled to a core which can be excited to various vibrational states. In general, the lowest lying states will be just the single particle states. At higher energies, the core can be excited to its first excited state, which, when coupled to the single particle state j, will give rise to a multiplet of states having $J = j + 2, j + 1, \ldots j - 2$. The center of gravity of this multiplet should have an energy $\hbar\omega$, that is, the energy of the vibrational phonon. Similar results are also possible for higher excitations of the core. Possible experimental evidence for such a coupling scheme has been examined by de-Shalit.[16]

Intermediate to these situations, the problem is apparently much more complex due to the mixing of single particle states due to the interaction with the core. Calculations have been made, for example, by Choudhury,[17] by Glendenning[18] and by Bannerjee and Gupta[19] for specific nuclei with a limited number of particle configurations. The applicability of such calculations is not clear at the present time due to lack of comparison with experimental data.

I.E. Residual Interactions

The models discussed above, engendering both particle and

collective features of the nucleus, have effectively replaced the particle interactions by a potential which is, in general, time dependent and non-spherical. This potential cannot take into account the entire interaction between the particles and a weak interaction can still be assumed to exist. Utilizing techniques introduced in superconductivity theory, Belyaev[20] studied the effect of a pairing force between the particles and found that the inclusion of this force could explain the energy gap (i.e., the absence of excited states below ~ 1 MeV) observed in even-even nuclei. The calculations were extended by Kisslinger and Sorenson[21] (KS) who included, in addition to the pairing force, a long range quadrupole interaction. These two forces have somewhat opposing effects, the pairing interaction tending to couple nucleons to zero angular momentum producing a spherical shape while the quadrupole force tends to correlate the motion of the nucleons giving rise to collective features (quadrupole vibrations) in the energy level spectrum. The resultant wave functions for the nuclear states are therefore a linear combination of particle and particle plus phonon wave functions. These authors have calculated many nuclear properties for nuclei from nickel to lead, not including the strongly deformed region $150 \leq A \leq 190$. The agreement with experiment is, in many cases, very impressive. For example, in the even-even isotopes, the agreement between theoretical and experimental reduced electric quadrupole transition probabilities, i.e., the B(E2) values, is usually within a factor of two. The predictions for the odd mass isotopes are even more interesting. The experimental electric

quadrupole moments of many such nuclei are an order of magnitude greater than the single particle prediction, whereas the values calculated by KS are in considerably better agreement. As might be expected, the states which have large phonon contributions are usually connected by particularly fast E2 transitions, in agreement with many of the observed transition rates. However, the agreement between observed and calculated M1 transitions, as pointed out by Geiger, et al.,[53] is generally somewhat less impressive.

Although the discussions given here do not exhaust the various models which have been tried in predicting nuclear levels and their properties, they may serve to indicate the types which have been found to give results bearing at least some resemblance to the experimental data.

Of particular interest for the experimental results to be reported here are the calculations of KS. The work by Bannerjee and Gupta,[19] which is concerned with energy levels in the iodine isotopes, will also need to be considered.

CHAPTER 2

SOURCE PRODUCTION AND PREPARATION

The radioactive isotopes employed in these studies were produced by either charged particle or thermal neutron irradiation of stable isotopes. The first nuclide to be studied, ^{121}Sb, is populated in the 154 day and 17 day electron capture decay of ^{121m}Te and ^{121}Te, respectively. These were produced by irradiating natural antimony metal, 57 percent ^{121}Sb and 43 percent ^{123}Sb, with 10 MeV protons and 20 MeV deuterons in the Brookhaven National Laboratory Cyclotron.

The powdered antimony metal was packed into a ~1/4" w. x 1/32" dp. x 3" long slot milled into a water cooled aluminum target and covered with ~10 mils of aluminum. Typically, irradiations of 200 to 400 microampere hour were required to obtain sufficient activity. Another ^{121}Te source, produced by thermal neutron irradiation of enriched ^{120}Te, was placed at our disposal by Dr. G. B. Beard of Wayne State University.

In order to reduce the contamination from other elements (and also to remove the inactive antimony from the cyclotron targets) the sources were chemically purified. The technique was essentially that given by Fink, et al.[23]

The levels in ^{123}Sb and ^{125}Sb were populated by the negaton decay of 125 day ^{123}Sn and 9.7 day ^{125}Sn, respectively. These parent nuclides were produced by irradiation of 10 mg quantities of ^{122}Sn and ^{124}Sn enriched to 94 to 96 percent. The irradiations were carried out in the ORR reactor at the Oak Ridge National

Laboratory for periods of one or two weeks in a thermal neutron flux of approximately 2 x 10^{14} n/cm^2 sec. These sources were chemically purified using a technique given by Newton and McDonnell.[24]

The last nucleus to be studied, ^{127}I, is fed in both the electron capture decay of ^{127}Xe and the negaton decay of ^{127}Te. However, only the latter decay populates the higher energy states and was therefore chosen for this study. The ^{127}Te was produced by thermal neutron irradiation of 10 mg samples of 94 percent enriched ^{126}Te in the ORNL research reactor for a period of two weeks. The target was chemically separated using the same technique referred to in the case of ^{121}Te. The main contaminants in this source were found to be ^{124}Sb and ^{110}Ag. After repeating the chemistry several times, no trace of these contaminants could be found in the source.

Two types of mounts were used in preparing a source for counting: for singles counting on an NaI(Tl) detector, where it is desirable to use a source geometry which is easily reproducible, the source was dried on a microscope slide cover glass and mounted in an aluminum frame by means of Scotch tape. These frames fit into an aluminum holder and could be readily interchanged with standard sources mounted in a similar way. For angular correlation measurements, liquid sources are used to reduce the possibility of perturbing the correlation (e.g., see Chapter 4.D.iii.). Therefore, the sources were contained in thin walled Teflon cups made by drilling a 1/8" x 1/2" hole in one end of a 1/4" x 1" length of Teflon rod. A 5/8" length of the drilled end was then

turned to make the walls as thin as practicable (approximately 5 to 10 mils).

CHAPTER 3

EXPERIMENTAL APPARATUS AND TECHNIQUES

The energy levels in the four isotopes ^{121}, ^{123}, ^{125}Sb and ^{127}I were studied using β- and γ-ray spectrometry. The experimental apparatus and techniques were more or less identical in the four investigations and are therefore described here only.

The bulk of the gamma ray singles and coincidence work was performed using NaI(Tl) scintillation detectors. These detectors were commercially packaged (Harshaw Chem. Co.) and were of two basic sizes. For high energy photons ($\geq$ 100 keV) detectors 7.6 cm diameter x 7.6 cm high were generally utilized. These represent a reasonable compromise between efficiency and resolution and are particularly convenient for use since extensive tables and curves of efficiencies and peak-to-total ratios are readily available.[25] Finite solid angle correction factors required in analyzing angular correlation data have also been calculated and measured for such crystals.[26] The crystals were originally mounted on Dumont type 6363 photomultiplier tubes using conventional mounting techniques.[27] The gain of these tubes proved to be very sensitive to both temperature and counting rate and were later replaced by EMI type 9578S photomultiplier tubes. The second type of NaI(Tl) detector used was designed to detect low energy photons ($\sim$6 to 100 keV). The NaI(Tl) crystals were 0.6 cm thick x 3.8 cm diameter and had windows of either 1 mil aluminum or 5 mil beryllium. These were mounted on either RCA 6342A or EMI 9536 photomultiplier tubes.

Both the large and small detector units proved to be quite

temperature sensitive and had to be kept at constant temperature ($\pm 0.5^{\circ}$ C). This was accomplished by performing most of the experiments with the apparatus inside a styrofoam box ($\sim 5' \times 5' \times 5'$) with the temperature being controlled by a bi-metallic regulator which operated a lightbulb used to provide heat. This proved to be a satisfactory low budget answer to a very serious problem. Gains stabilized in this way were found to be constant to within ± 0.5 percent over a period of several days.

In addition to NaI(Tl) photon detectors, a xenon-methane filled proportional counter (Amperex 300 PC) was used in one experiment. This detector has the advantage of reasonable resolution ($\sim$ 10-20 percent) in the energy range from $\sim$3 to $\sim$40 keV. However, it also has a serious disadvantage in its low efficiency.

In the later stages of the experimental work ($\sim$ Dec., 1964), a new type of gamma ray spectrometer became available which has created somewhat of a revolution in gamma (and particle) spectroscopy. These are the semiconductor detectors.[28] Thus far, only silicon and germanium crystals have been used successfully, with silicon being used primarily for particles and germanium for photons. Prior to the introduction of the germanium gamma ray detector (designated Ge(Li)) precision energy measurements had to be made on crystal diffraction spectrometers or in β-ray spectrometers using internal or external conversion. Both methods required, in addition to very expensive equipment, extremely intense sources. The Ge(Li) detectors used in these studies typically had a resolution of 5-6 keV for the 662.6 keV gamma rays from ^{137}Cs (compared to $\sim$50 keV for NaI(Tl)). The efficiencies of such

detectors have so far been rather small compared to NaI(Tl) detectors because of their small size and low Z. One detector, which has been used here, has a sensitive volume approximately 2 cm diameter x 4 mm deep. The photo efficiency vs. energy curve for this detector is shown in Figure 1. The standard intensities were obtained from a similar curve for NaI(Tl).[25]

In addition to the use of scintillation detectors as photon counters, similar detectors were used to study the electrons emitted in the decay of ^{123}Sn and ^{125}Sn. The detectors in this case were plastic (Naton 136). Two types of source-detector geometry were employed: In the case of ^{123}Sn, which will be seen later to have a very simple decay scheme, it was desirable to study not only the energies of the electrons but also the shape of the spectrum. Since considerable distortion can result from backscattering of electrons incident on the face of the scintillator, the source was sandwiched between two detectors and the unit mounted on an RCA 6342A phototube. The joint between the detectors was sealed with reflecting adhesive tape and aluminum foil wrapped around the detectors served as a light reflector. Good performance was obtained with this system down to electron energies $\leq$ 100 keV (as indicated by a study of ^{60}Co electrons[29]). The second configuration that was used, which is more convenient when only end point energies are desired and some distortion can be tolerated, was with the source external to the detector. Experiments of this type were used in the study of the decay of ^{125}Sn with a 2.5 cm thick x 5 cm diameter plastic scintillator with a 1.0 mg/cm^2 aluminized mylar window to reduce absorption and to

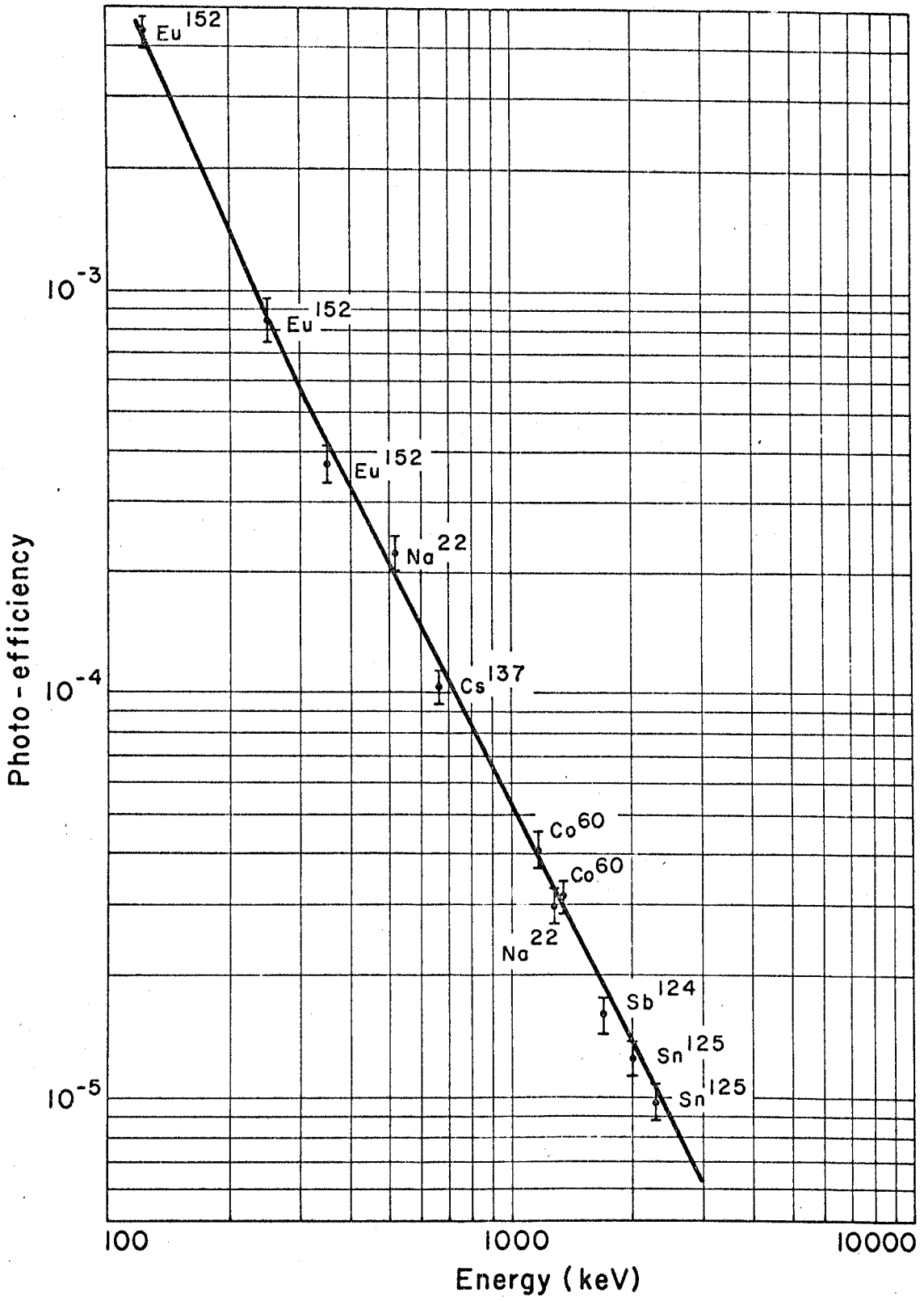

Figure 1. Photo-efficiency vs. energy for a 4mm x 2mm Ge(Li) detector.

provide good light collection efficiency.

The data taken with these detectors were of two types, singles and coincidence. Singles studies, applied here primarily to the study of the gamma-ray spectra, give the energies and intensities of many of the transitions but are usually insufficient for determining a unique level scheme. The analyses of the data are quite different for NaI(Tl) and Ge(Li) detectors. The resolution of the NaI(Tl) detector is generally insufficient to resolve the peaks in the spectrum and one must rely on spectrum stripping[25,30] to locate the weaker lines. In the Ge(Li) spectrum, on the other hand, the individual lines are usually well resolved, affording better energy and intensity measurements and obviating, in most cases, the need for spectrum stripping.

In order to aid in the construction of the decay scheme, coincidence relations between the radiations were studied. A fast-slow coincidence circuit (Cosmic Radiation Laboratories, Model 801) having a variable resolving time was used to gate the multichannel analyzer (MCA). The MCA used for most of the work (Nuclear Data 150 FM) had a 1024 channel memory and two-parameter analysis capabilities, which allowed the simultaneous study of spectra in coincidence with several gamma ray transitions.

In obtaining and analyzing coincidence data, one must usually record two spectra; one including both true and chance coincidences and a second containing only chance coincidences. The difference between the two is then taken to obtain the desired true coincidence spectrum. In order to eliminate the need for recording a separate chance spectrum, the analyzer was modified so

that an equivalent chance spectrum could be subtracted as the true plus chance spectrum is being recorded. This is accomplished as follows: The analyzer is normally programmed to "add-1" to an appropriate memory location whenever a pulse is analyzed. However, if the pulse is accompanied by a control signal, the analyzer automatically switches to the "subtract" mode and will "subtract-1" from the memory. Upon carrying out this one operation, the analyzer again returns to the "add" mode. The required control signal is obtained by the use of two coincidence circuits having identical resolving times, but one of which detects only chance coincidences. The coincidence output from the "chance-only" circuit is then used to control the mode of the MCA.

One of the main problems encountered in gamma-gamma coincidence studies was the existence of crystal-to-crystal Compton scattering, leading to false coincidences and distortion of the spectrum. In order to eliminate, or at least reduce, this problem, a scattering shield was designed to fit over the NaI(Tl) crystals (used in most of the gamma-gamma coincidence work). These consisted of two parts: a lead cylinder 10 cm I.D. x 15.5 cm O.D. x 15.5 cm long, and a lead cone whose inside dimension tapered from 10 cm to 1 cm while the outside diameter went from 15.5 to 3 cm. All surfaces were covered by 0.05 cm Cd or Sn and 0.05 cm Cu to absorb fluorescent Pb X-rays. The two detectors were normally placed at an angle of 90° and were therefore separated by $\sim$ 10 cm of lead. Even at 180°, very little scattering could be detected.

In addition to providing a clue as to the locations in the level scheme of lines strong enough to be seen in the singles spectrum, coincidence studies usually make it possible to observe additional weak transitions. This was found to be true in all of the decay scheme studies made here. Also, by measuring the coincidence rate as a function of angle between the detectors, that is, by studying the angular correlation of coincident gamma rays, one can usually learn something about the spins of the nuclear states and the character (dipole, quadrupole, etc.) of the radiations. A summary of angular correlation theory and methods of data analysis have been given previously.[31]

CHAPTER 4

EXPERIMENTAL RESULTS

4.A. The Decay of ^{121}Te and ^{121m}Te

4.A.i. The Gamma Ray Singles Spectrum

The gamma ray spectrum from the combined ^{121}Te and ^{123}Te activities is shown in Figure 2. The source was mounted 10 cm from a 7.6 x 7.6 cm NaI(Tl) crystal, the unit having a resolution of 8.7 percent for the 662 keV photopeak from ^{137}Cs. The relative intensities were obtained using line shapes obtained by interpolation between spectra from standard sources. These were taken with the same geometry and approximately the same counting rates as were used in obtaining the tellurium spectrum.

The peaks at 160 and 214 keV are from known isomeric transitions in ^{123}Te and ^{121}Te, respectively.[22,33] The 506, 572 and 1102 keV lines had been reported by previous investigators[33] in addition to a 68 keV transition which is obscured by the Compton distribution from the intense higher energy transitions. By placing a graded lead absorber over the face of the crystal to absorb most of the 160 and 214 keV photons, it was found that the peaks at 730 and 790 keV were due to the accidental summing of the 572 with the 160 and 214 keV photons.

However, the absorbers changed the ratio of the 910 and 1000 keV to 1103 keV peak heights only by an amount consistent with the difference in absorption coefficients of the three photon energies. In addition, these peaks were found with the same relative intensities, within experimental error, in four

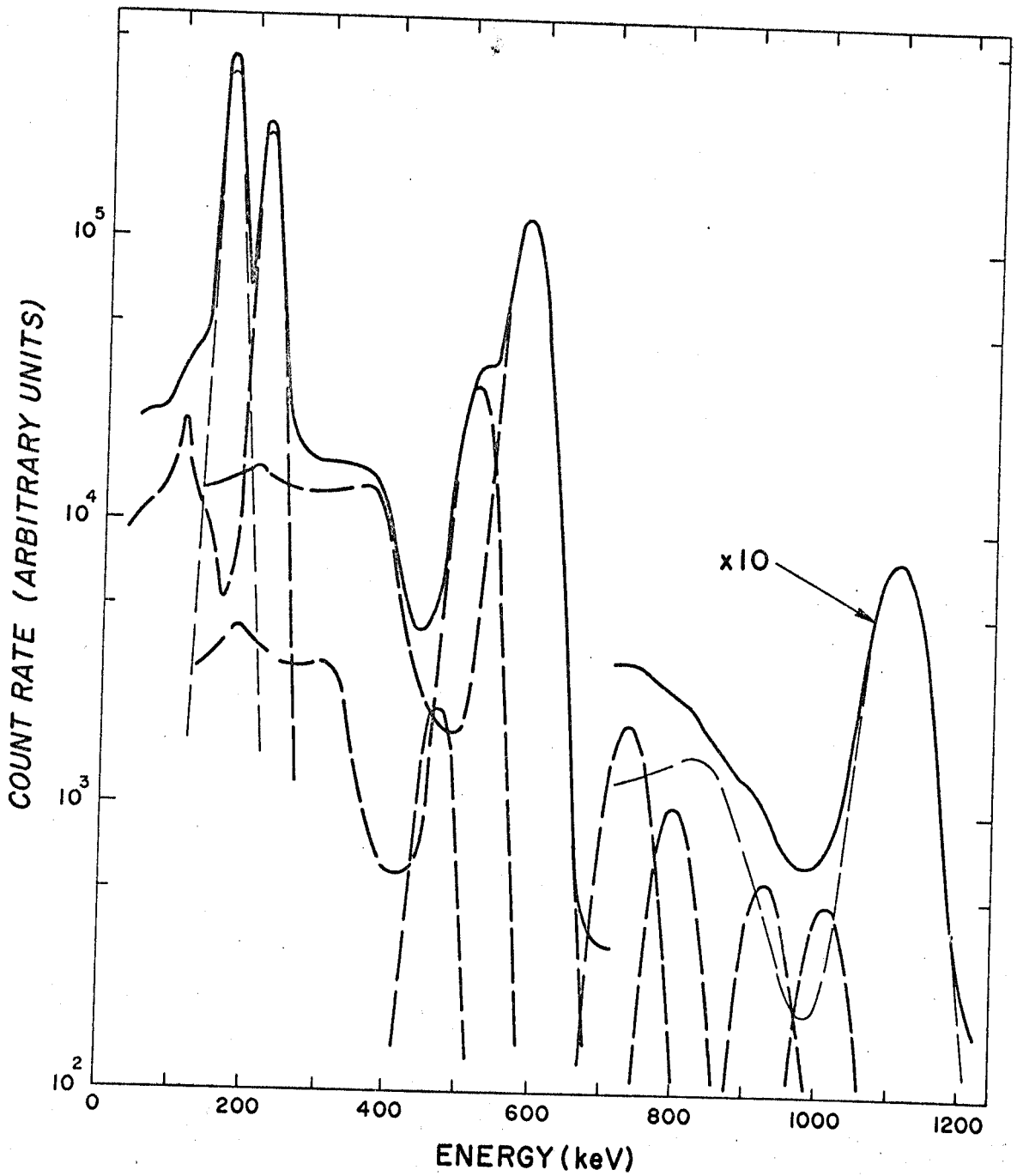

Figure 2. The gamma ray singles spectrum of ^{121}Te plus ^{123}Te.

different sources. Of the sources used, three were from proton or deuteron bombardments, while the fourth was the neutron produced source. The consistency, both in energy and intensity, with which the 910 and 1000 keV lines are found, regardless of the mode of source production and despite repeated chemical separations, is believed to be strong evidence that these transitions are in the decay of ^{121}Te. In addition, the decay of the source was followed for several months and all of the peaks , with the exception of that at 160 keV, were found to decay with the same halflife.

4.A.ii. Coincidence Studies

The spectrum in coincidence with the unresolved antimony and tellurium K-X-ray peaks is shown in Figure 3. Two NaI(Tl) crystals with axes at 90° were employed with the source 10 cm from both crystals. The spectrum was corrected for chance coincidences by delaying the signals from one of the detectors. When the singles spectrum was superimposed on this coincidence spectrum and normalized on the 572 keV photopeak, it was found that the 910, 1000 and 1102 keV peaks were enhanced in the coincidence spectrum by a factor of 1.96 $\pm$ 0.06. Since the theoretical K to L capture ratio is essentially the same for capture to the high energy states as it is for capture to the 572 keV state, this would indicate that the 910, 1000 and 1102 keV transitions are in coincidence with a highly converted transition. In order to give the observed enhancement, this transition must have a K-shell conversion coefficient $>$ 9. Assuming that this transition

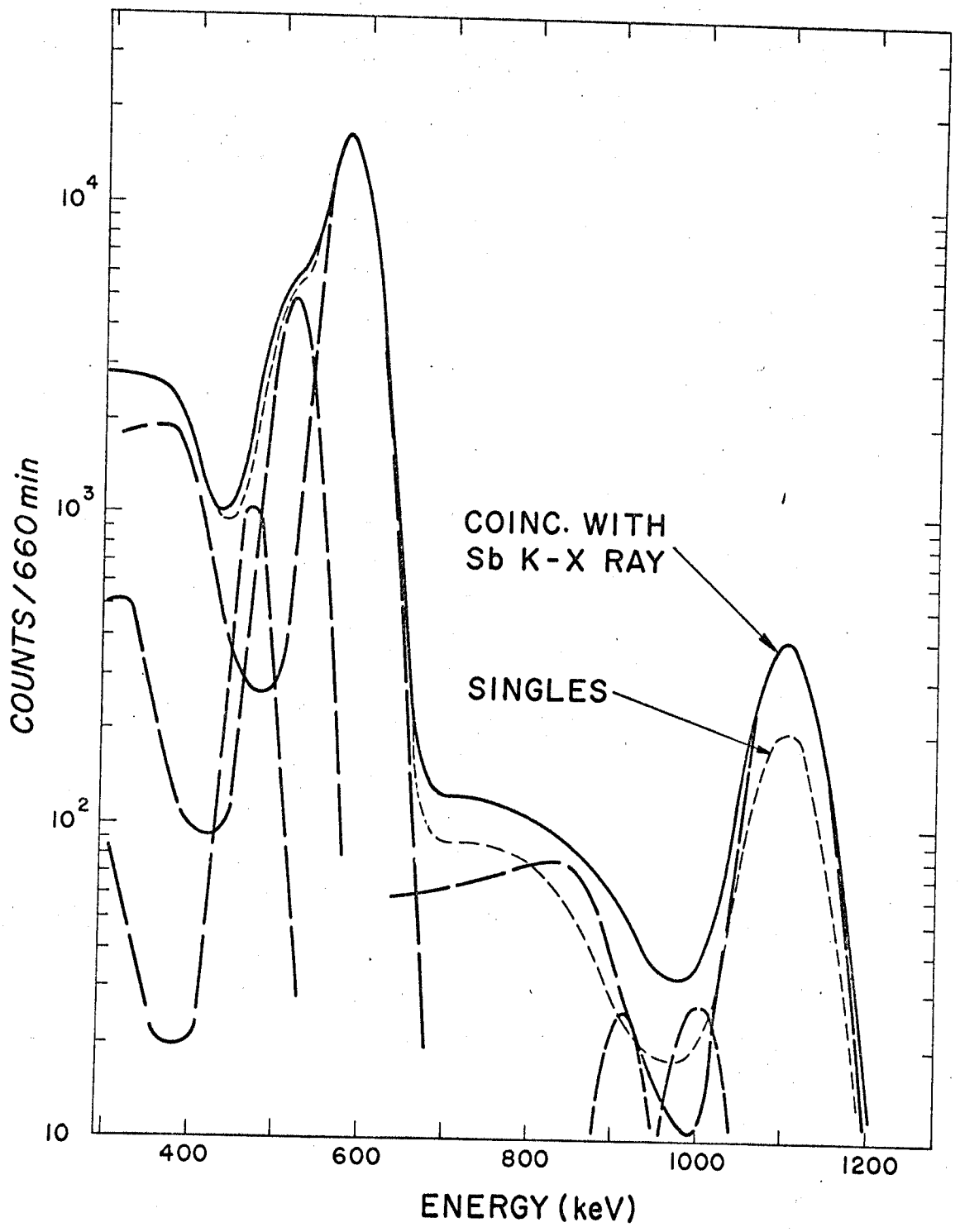

Figure 3. K X-ray-gamma coincidence spectrum of ^{121}Te.

is from the low lying $7/2^+$ state of ^{121}Sb predicted by the shell model and expected from level systematics, one would expect the radiation emitted to be primarily M1. Under this assumption, a K shell conversion coefficient of 9 suggests that the energy of the transition be about 30 keV.

It was also found that the 506 keV peak is only slightly enhanced in the coincidence spectrum. This indicates that the low intensity of the 68 keV transition cannot be explained by a high conversion coefficient and that it must therefore precede the 506 keV photon.

The 470 keV region was also found to be enhanced in the coincidence spectrum showing that there is a 470 keV transition which is also in coincidence with this highly converted transition. This lends support to the assumption that the ~30 keV transition is from the first excited state since the 470 keV will be shown later to be in coincidence with the 68 keV transition and therefore probably connects the 506 and ~30 keV states.

The energy of the converted transition discussed above was determined by observing coincidences between 1102 keV photons and the low energy portion of the gamma spectrum. The xenon-methane filled proportional counter was employed as the low energy detector while the 1102 keV photons were detected by a NaI(Tl) crystal (unless indicated otherwise, the NaI(Tl) detector used is the 7.6 cm x 7.6 cm unit). The detectors were 180° apart with the source 1.0 cm from the proportional counter and 10 cm from the high energy detector. Approximately 0.03 cm of polyethylene, placed between the source and proportional counter, was

used to stop the conversion electrons from the highly converted transitions. Due to the low efficiency of the proportional counter and the high conversion coefficient of the low energy transition, the experiment had to be extended over a period of several days. However, frequent gain checks showed that drifts were negligible (< 1 percent).

The results shown in Figure 4 indicate that the 1102 keV transition is in coincidence with a 38 ± 2 keV transition as well as Sb K_{α}-, K_{β}-, and L- X-rays at 26.2, 29.7 and 3.6 keV, respectively. The improved resolution of the Sb K_x- ray lines is due to the absence in the coincidence spectrum of the Te K_{α} X-ray. The peak at 6.5 keV is due to Fe K-X-rays arising from scattering in the stainless steel body of the proportional counter and the peak at 11.4 keV is due to a small amount of selenium carrier remaining in the source. The enhancement in the 16 to 22 keV region is believed to be due primarily to Compton scattering and, to a lesser degree, to Xe L-X-ray escape. The chance coincidence spectrum was found to have the same shape as the singles spectrum which is shown for comparison.

The coincidence data and the 1102 keV singles intensity indicate that approximately 2 percent of the 1102 keV photons were in coincidence with 38 keV photons. This is an agreement with the high conversion coefficient suggested by the K-X-ray coincidence data. Monaro, et al.,[34] have published an account of lifetime measurements on the 38 keV transition which confirms our placing this transition from the first excited state of ^{121}Sb. They find the half life of the 38 keV state to be 3.5 ± 0.2 nsec

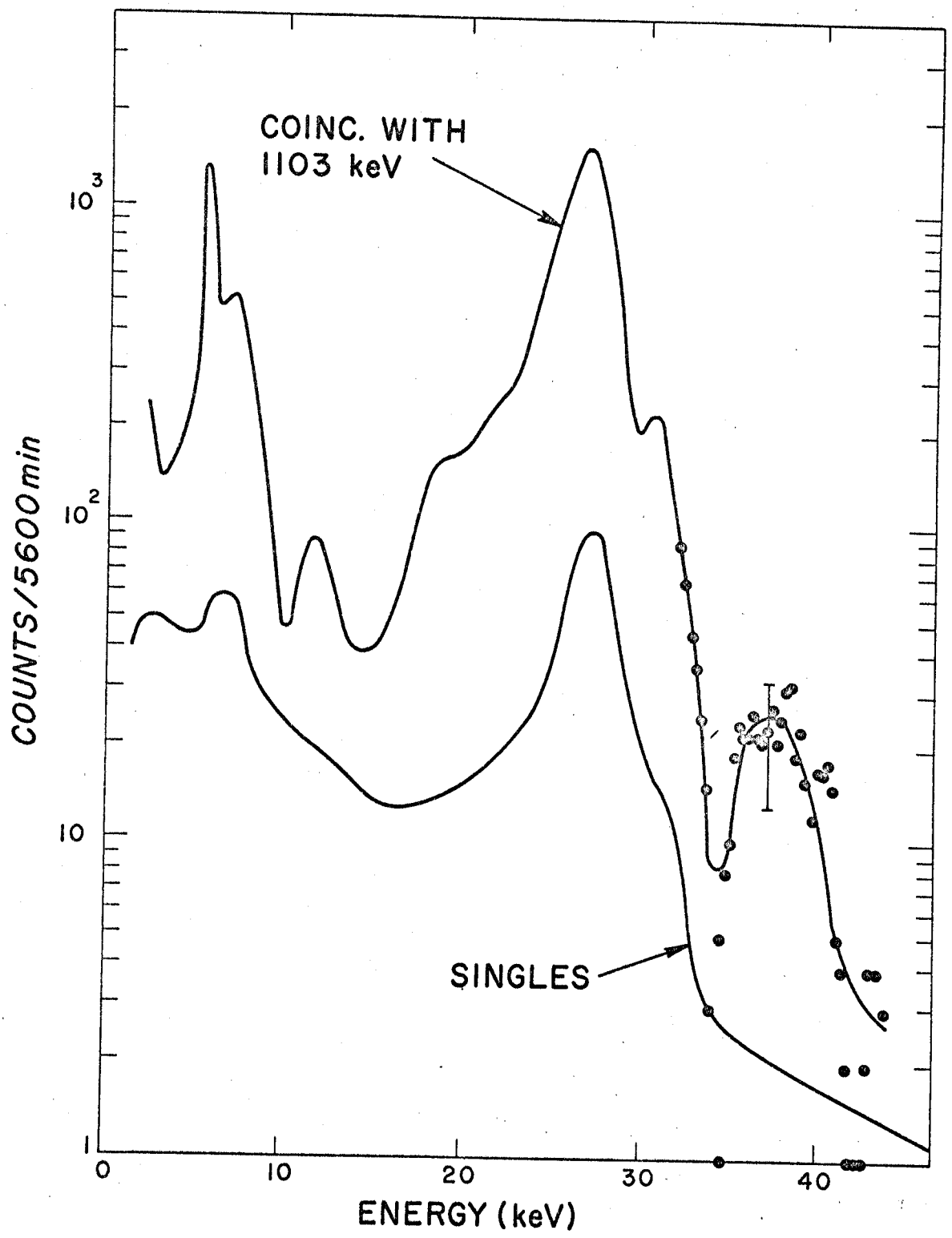

Figure 4. Low energy photon spectrum in coincidence with the 1102 keV transition in ^{121}Te.

and assign the transition to be a probable M1. Beard and Snyder have recently observed this 38 keV transition accompanying the negaton decay of ^{121}Sn and have performed Mossbauer experiments on it.[35]

A two parameter analysis was made of coincidences between photons in the 25 to 150 keV region and the 700 to 1100 keV region using the 64 x 16 channel mode of the 1024 channel analyzer. Two NaI(Tl) detectors were employed to detect the photons, with the crystals at 90° and anti-scattering shields in place. The results are shown in Figures 5 and 6. Figure 5 shows the high energy portion of the spectrum in coincidence with photons from 80 to 120 keV. The dashed line shows the chance coincidence contribution. Figure 6 is the low energy region in coincidence with photons in the 970 to 1040 keV region. These data indicate that the 1000 keV transition is in coincidence with a transition having an energy of 103 keV. The only low energy coincidences obtained with the remainder of the high energy region were with K-X-rays, the 38 keV peak being obscured by the intense X-ray peak.

A study was also made of the 150-300 keV region in coincidence with the 700-1100 keV region. Any coincidences, if present, were masked by chance coincidences with the intense 160 and 214 keV photons.

The 103 keV photon intensity, determined from the 1000-103 keV coincidence and 1000 keV singles count rates, was found to be approximately 10 percent of the 1000 keV photon intensity. Since the 103 keV transition is not highly converted, as evidenced by

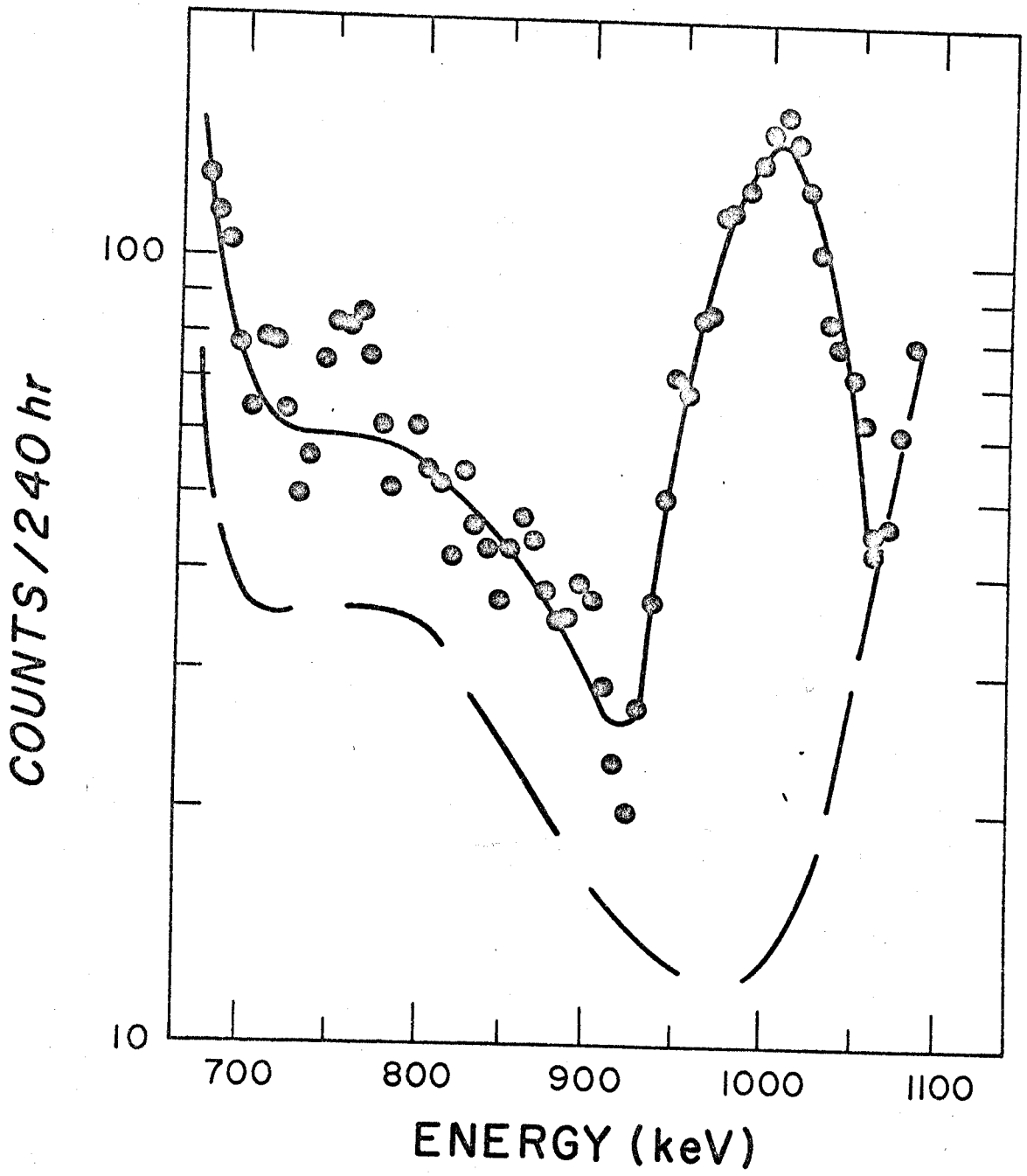

Figure 5. The high energy gamma spectrum in coincidence with the photons in the 80 to 120 keV region of the ^{121}Te gamma spectrum.

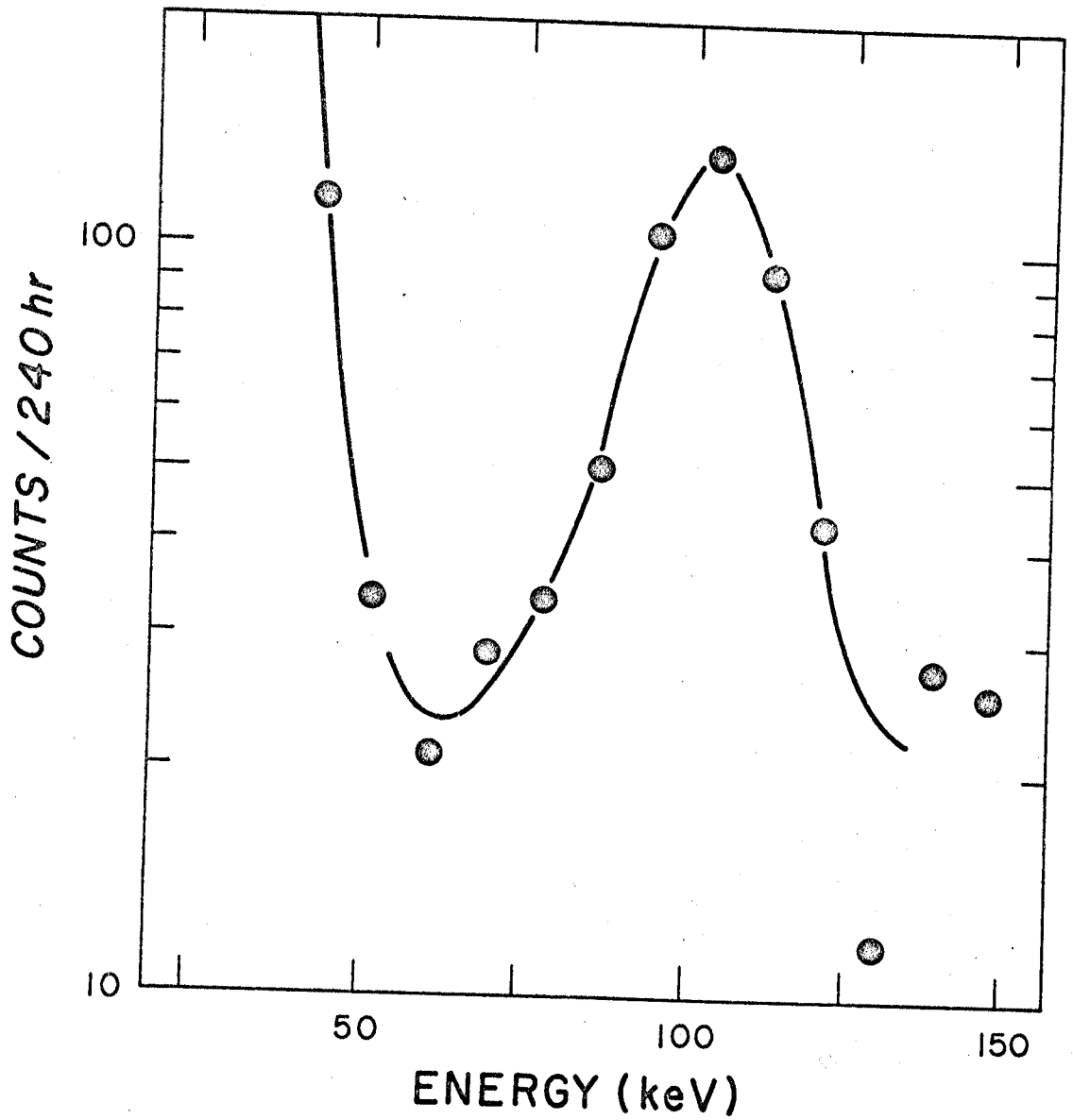

Figure 6. Spectrum in coincidence with the 970-1040 keV region of the ^{121}Te spectrum.

the similar enhancements for the 1102 and 1000 keV transitions in coincidence with the K-X-rays, its low intensity requires that it precede the 1000 keV transition.

As already noted, the 506 keV transition is in coincidence with a 68 keV transition. However, when the analyzer was gated on the 68 keV region, it was found that the 470 keV region, as well as the 506 keV peak, was enhanced in the coincidence spectrum and that the relative intensities of the 470 and 506 keV peaks remained essentially the same as in the singles spectrum. A search of the high energy region (> 572 keV) was made, and no coincidences with the 68 could be found as had been reported by other groups.[36]

The angular correlation between the 68 and 506 keV photons was measured using two NaI(Tl) detectors enclosed in scattering shields. The source, in which the 17 day and 154 day activities were essentially in equilibrium, was in liquid form and located 12 cm from both detectors. The lead cones used for shielding extended to within 2 cm of the source. The multiparameter feature of the multichannel analyzer was used to obtain an accurate correction for the close lying, intense K-X-ray peak. Small corrections for source decay and source asymmetry were made and the least squares coefficients computed and corrected for detector solid angle.[31] The result obtained was $W(\theta) = 1 + (0.066 \pm 0.009)P_2(\cos\theta) + (0.00 \pm 0.02)P_4(\cos\theta)$. This result is consistent with a 3/2 assignment for the 506 keV state and either 1/2 or 3/2 for the 572 keV state. However, the mixing ratio for the 506 keV transition has been determined recently to be

(E2/M1) = +0.29 ± 0.09 from angular distribution measurements on nuclear resonance fluorescence.[37] Using this value, it was found that only two cases were possible: a) spin sequence 3/2, 3/2, 5/2 with a 68 keV mixing amplitude $\delta = -0.34 \pm 0.02$; and b) spin sequence 1/2, 3/2, 5/2 with a 68 keV mixing amplitude $\delta = +0.17 \pm 0.03$. These give E2 to M1 mixing ratios of $\delta^2 = 0.11 \pm 0.01$ and 0.03 ± 0.01 for a) and b), respectively. Recent conversion electron measurements[38] show that for the 68 keV transition $\delta^2 \leq 0.02$, thus the only spin sequence and mixing ratio which is consistent with all available data is case b), requiring a spin assignment of 1/2 for the 572 keV state.

The question[39] of possible positon branching in the decay of ^{121}Te has been studied by detecting 511-511 keV photon coincidences for various angles from 90° to 180°. An extremely weak annihilation radiation was found to exist, since coincidences were found at 180° but not at 90° or 135°. An estimate of the positon branching which would be necessary to account for the observed annihilation radiation was obtained from the coincidence data and found to be approximately 0.003 percent of the total ^{121m}Te decay. The possibility of pair production from the 1102 keV photons was studied and could account for less than 10 percent of the observed annihilation radiation. Attempts to determine which states are fed by the positon decay and to measure the end point energy were unsuccessful due to the extremely low intensity of the transition.

4.A.iii. Summary of ^{121}Te Results

The results of these measurements on ^{121}Te are summarized in Table 1. The relative photon intensities given for the 214, 470, 506, 572, 910, 1000 and 1102 keV transitions were obtained from singles spectra with corrections being made for the net detector efficiencies and the peak to total ratios.[25] The 68 keV intensity was calculated from the 68-506 keV coincidence data and the 103 keV intensity was obtained from the 103-1000 keV coincidence measurements.

The equilibrium transition rates were determined by making photon emission rate measurements on a source in which the 17 day component had essentially decayed out, so that only a small correction was necessary to obtain the equilibrium transition rates. It was found that the K-X-ray emission rate could not be completely explained by the transitions discussed above and the highly converted isomeric transitions in ^{121}Te and ^{123}Te. This was to be expected to some extent since the K-capture to positon-emission ratio is expected to be approximately 1000 for transitions from ^{121m}Te to the 38 keV state of ^{121}Sb (which is the only position in the decay scheme which can be assigned to the observed positon transition). The electron capture branching to the 38 keV state required to account for the high X-ray intensity is approximately 16 percent, which is a factor of ~ 5 larger than the feeding expected from the positon intensity and theoretical capture to positon ratio. This may indicate that additional highly converted transitions are present which have gone unobserved.

The decay scheme proposed on the basis of these results is

Table 1. Summary of the results of measurements on photons emitted in the decay of the ^{121}Te isomers.

Transition Energy (keV)	Relative Photon Intensities	Equilibrium Transition Rates[a]	Coincident Transitions[c], keV
K-X-ray		117	
214 ± 2 I.T.	100	81	
1102 ± 2	3.4 ± 0.1	2.6	38
1000 ± 5	0.11 ± 0.02	.085	(38), 103
910 ± 40	0.1 ± 0.05	.08	(38)
103 ± 4	0.02 ± 0.01	.008	1000
38 ± 2		20[b]	(470,910,1000) 1102
572 ± 5	100	65	
506 ± 5	23 ± 1	14.7	68
470 ± 5	1.8 ± 0.3	1.16	68, (38)
68 ± 2	0.5 ± 0.1	0.96	506, 470

[a] Absolute transition rates for the case where the 154 day and 17 day states are in equilibrium and normalized to 100 decays of 154 day ^{121m}Te. Correction for internal conversion was made by assuming the transitions are pure multipoles of lowest order consistent with the proposed decay scheme. Theoretical conversion coefficients were taken from tables by Rose[40] and by Band and Sliv[40a] The X-ray rate is the number of K-X-rays obtained per 100 decays of 154 d ^{121m}Te.

[b] Based on the assumption that the high X-ray count rate is due to direct capture from ^{121m}Te to the 38 keV state of ^{121}Sb.

[c] Those transition energies given in parentheses are inferred from coincidence measurements with the K-X-ray.

shown in Figure 7. The arguments for the given time ordering of the transitions are as follows: i) the 68 keV transition must precede the 506 in order to explain its low relative intensity since the X-gamma coincidence results rule out the possibility of a high conversion coefficient. This time ordering is in agreement with the nuclear resonance fluorescence measurements of Metzger and Langhoff.[37] ii) Since the 38 keV transition is in coincidence with both the high energy (910, 1000 and 1102 keV) and the 470 keV transitions, and since the 470 keV transition is also in coincidence with the 68 keV transition, the 38 must follow these transitions. This is in agreement with the results of other recent investigations.[34,38] iii) The low relative intensity of the 103 keV transition suggests that it precedes the 1000 keV transition and that there is direct capture to the 1038 keV state.

The spin assignments 1/2 and 3/2 for the 572 and 506 keV states, respectively, are required by the results of the measurement of the angular correlation between the 68 and 506 keV photons.

The log ft values[41] given in Figure 7 were obtained assuming the ground states of ^{121}Te and ^{121}Sb are separated by approximately 1300 keV.[32] This value is from nuclear systematics. The log ft values found for the electron capture transitions to the 572 and 506 keV states indicate that these are allowed transitions and are therefore in agreement with the above spin assignments. The allowed nature of these transitions also indicates that the 506 and 572 keV states have positive parity. The $7/2^+$ assignment for the 38 keV state is based on shell model predictions and energy level systematics and is in agreement with the recent lifetime

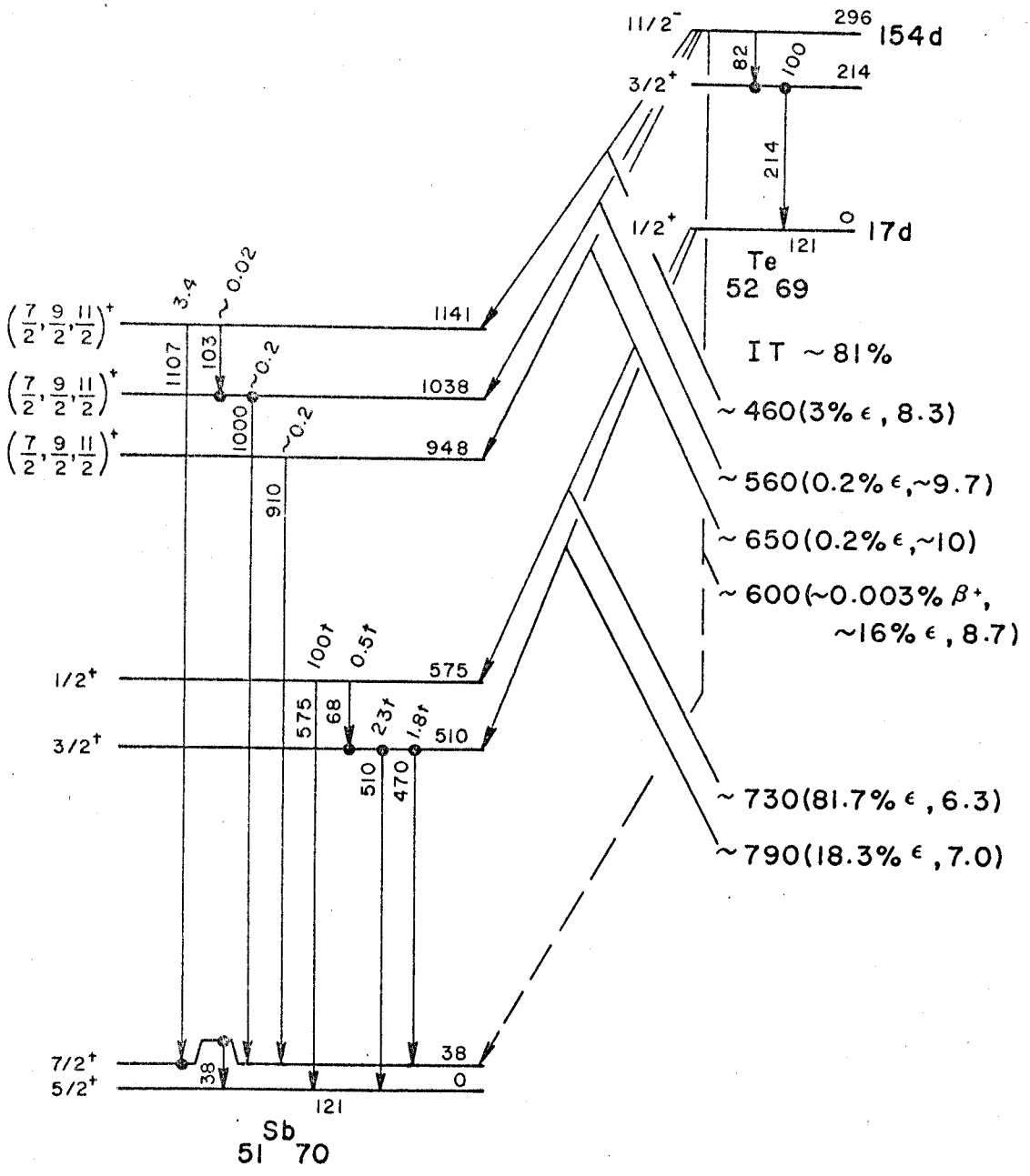

Figure 7. The proposed decay scheme of ^{121}Te and ^{121m}Te.

measurement of this state by Monaro, et al.,[34] and the approximate internal conversion coefficient given above. The log ft values for capture to the 1140 and 1038 keV states indicate first forbidden transitions and suggest spins of $7/2^+$, $9/2^+$ or $11/2^+$ for each of these states. The mode of feeding the 948 keV state has not been determined and has tentatively been assigned direct feeding from ^{121m}Te on the basis of log ft values.

4.B. The Decay of ^{123m}Sn

4.B.i. The Singles Spectra

The gamma-ray spectra were studied using both NaI(Tl) and Ge(Li) detectors. The spectrum obtained with the NaI(Tl) detector is shown in Figure 8. This spectrum was taken with a 3 mm thick lead absorber to reduce chance summing of the high energy photons with the much stronger 392 keV line[42] from ^{113}Sn. The source was also sandwiched between 7 mm thick carbon absorbers to reduce bremstrahlung from the intense beta radiation. The high energy line has been stripped using a peak shape interpolated from lines in ^{65}Zn (1115 keV) and ^{207}Bi (1063 keV). This shows that the high energy "peak" actually contains lines from two transitions.

The energies and intensities of these transitions were measured with the Ge(Li) detector, the spectrum from this detector being shown in Figure 9. The energies were found to be 1089 ± 1 and 1032 ± 1 keV, with the intensity of the latter being 0.056 ± 0.006 times that of the first.

The small peak at 428 keV is due to ^{125}Sb (from the decay of ^{125}Sn) and the intense lines at 392 and 255 keV are from ^{113}Sn.

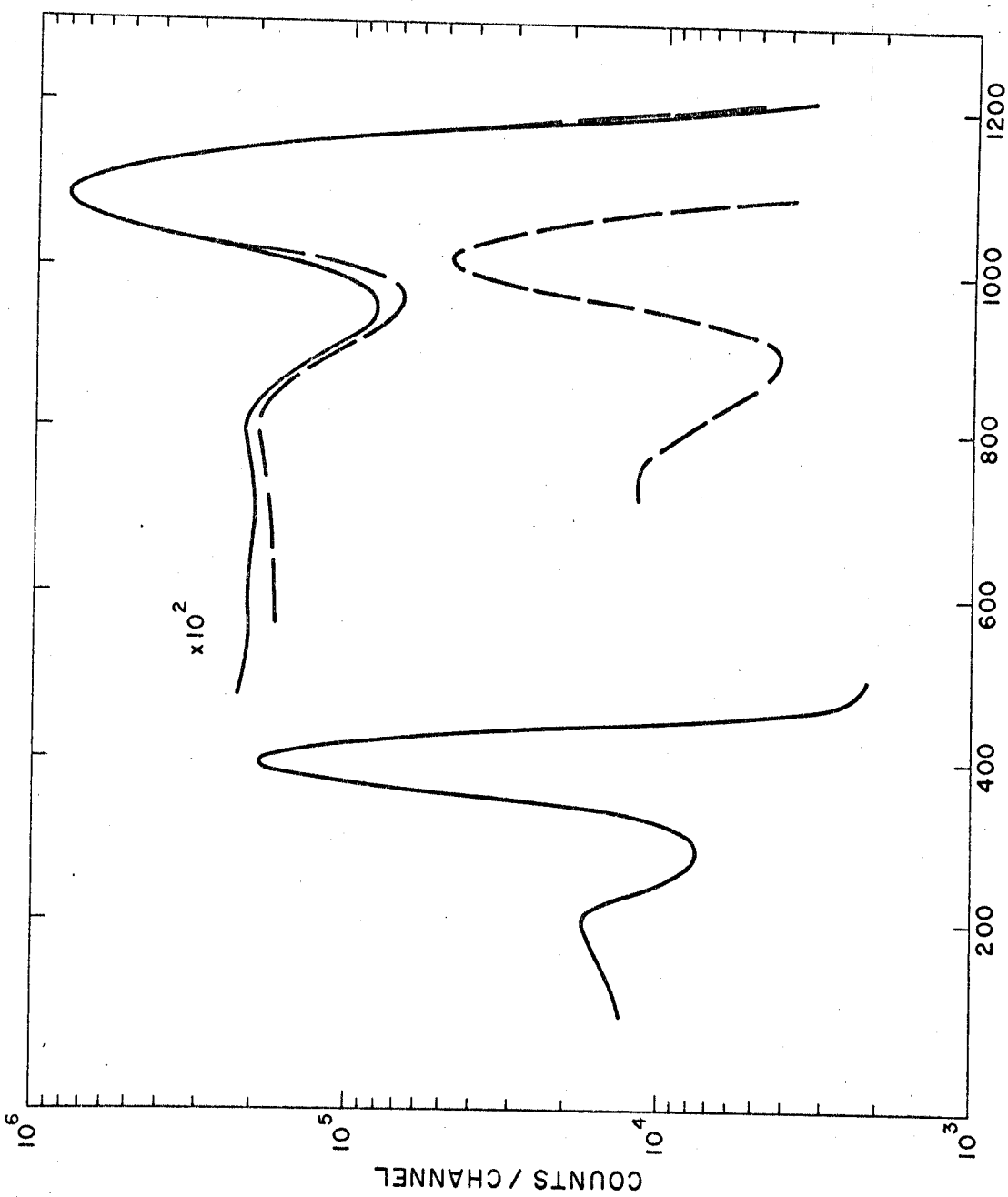

Figure 8. Singles gamma ray spectrum of ^{123}Sn (125 d) plus ^{113}Sn obtained with a NaI(Tl) detector.

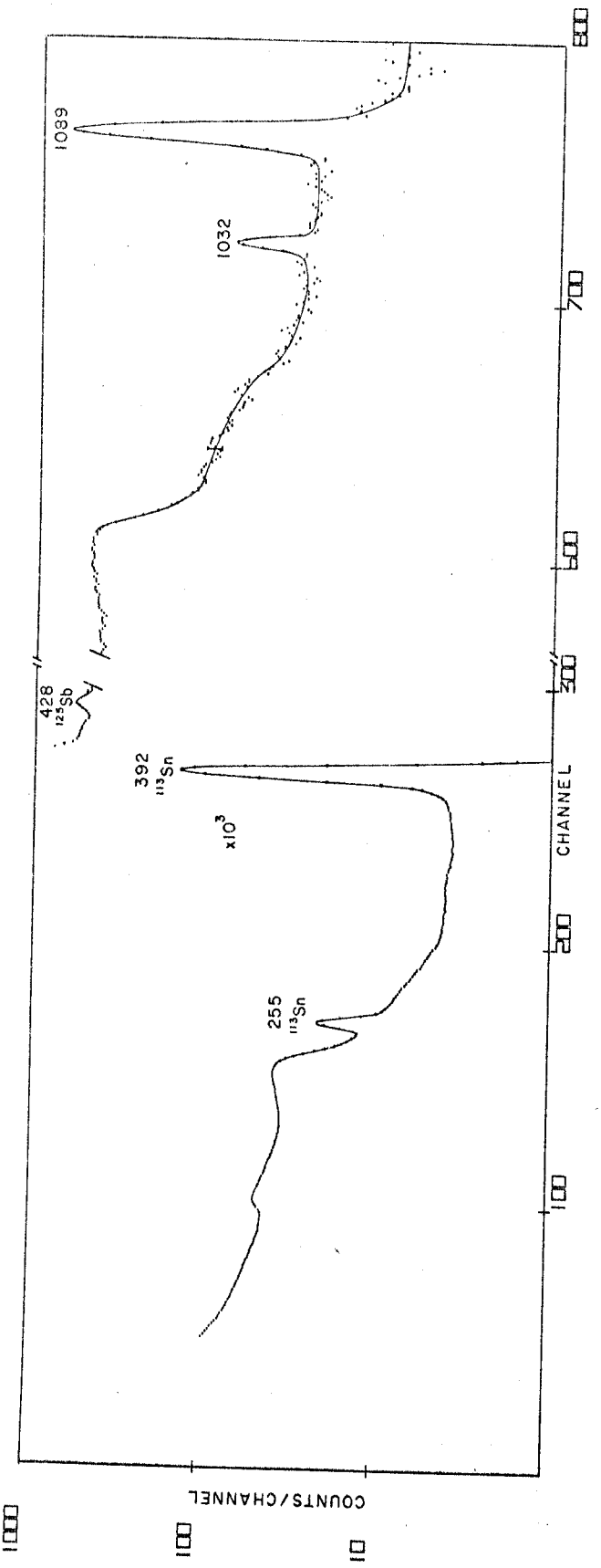

Figure 9. Gamma spectrum of ^{123}Sn (125 d) plus ^{113}Sn obtained with a 4mm by 2cm Ge(Li) detector.

The relative intensities of the 1032 and 1089 keV peaks were studied over a period of 7 months and it was found that the two transitions decayed with the same half life, in agreement with the assignment of the 1032 keV transitions to ^{123}Sn.

4.B.ii. Coincidence Studies

In order to determine if additional low intensity transitions could be detected, coincidence measurements were made. All regions of the spectrum were studied, with particular attention being paid to coincidences with the 160, 380, and 540 keV regions. These are regions in which transitions had been observed in the decay of the low spin ($3/2^+$) isomer of ^{123}Sn or in Coulomb excitation studies.[43] In addition, the 1032-1089 keV region also received careful study. In only one case was a positive result obtained, that being with the gate on the low energy side of the 1032-1089 keV peak. With the gate set on this region, a very weak line was observed at 155 ± 10 keV. When the gate was moved to the high energy side of the peak, this line did not appear.

These results are interpreted as indicating a coincidence between the 1032 keV transition observed in the singles spectrum and a 155 keV transition having a relative intensity of approximately 4 percent of the 1032 keV intensity. The intensity was deduced from singles and coincidence counting rates and tables of detector efficiencies and peak to total ratios.[25] Since the 155 keV transition is not highly converted, as indicated by the absence of K-X-ray-gamma coincidences, this low intensity suggests that it precedes the 1032 keV transition, thus requiring a state

at ~1187 keV.

4.B.iii. Beta Spectrum Studies

Although the shape of the transition to the ground state of ^{123}Sb had been measured and found to be consistent with $\Delta J^{\Delta\pi} = 2^{yes}$, no information was available on the β transitions to the excited states. It was soon evident from the measured relative intensities of the gamma transitions that only the 1089 keV level was populated with sufficient strength to allow one to make any meaningful beta-gamma coincidence measurements. Due to the high relative intensity of the ground state beta transition, very weak sources had to be used in the beta detector. The 4π electron detector described in Chapter 3 was used to reduce the effects of backscattering. The gamma detector was a 7.6 cm x 7.6 cm NaI(Tl) crystal at 180° with the plastic scintillator. A 3 mm thick graded lead absorber was placed over the face of the NaI(Tl) detector to reduce the number of backscattered photons entering the two crystals.

The spectrum obtained was corrected for detector resolution[44] and a Fermi-Kurie plot obtained.[45] This plot is shown in Figure 10 and indicates that the spectrum has an allowed shape. This would indicate that the transition is allowed or non-unique first forbidden.[45] The energy calibration was obtained from Compton edges of several standard gamma transitions and K-conversion electrons from the 392 keV transition in ^{113}Sn (gating on the K-X-ray in the NaI(Tl) detector). The end point of the spectrum was found to be 330 $\pm$ 10 keV, in good agreement

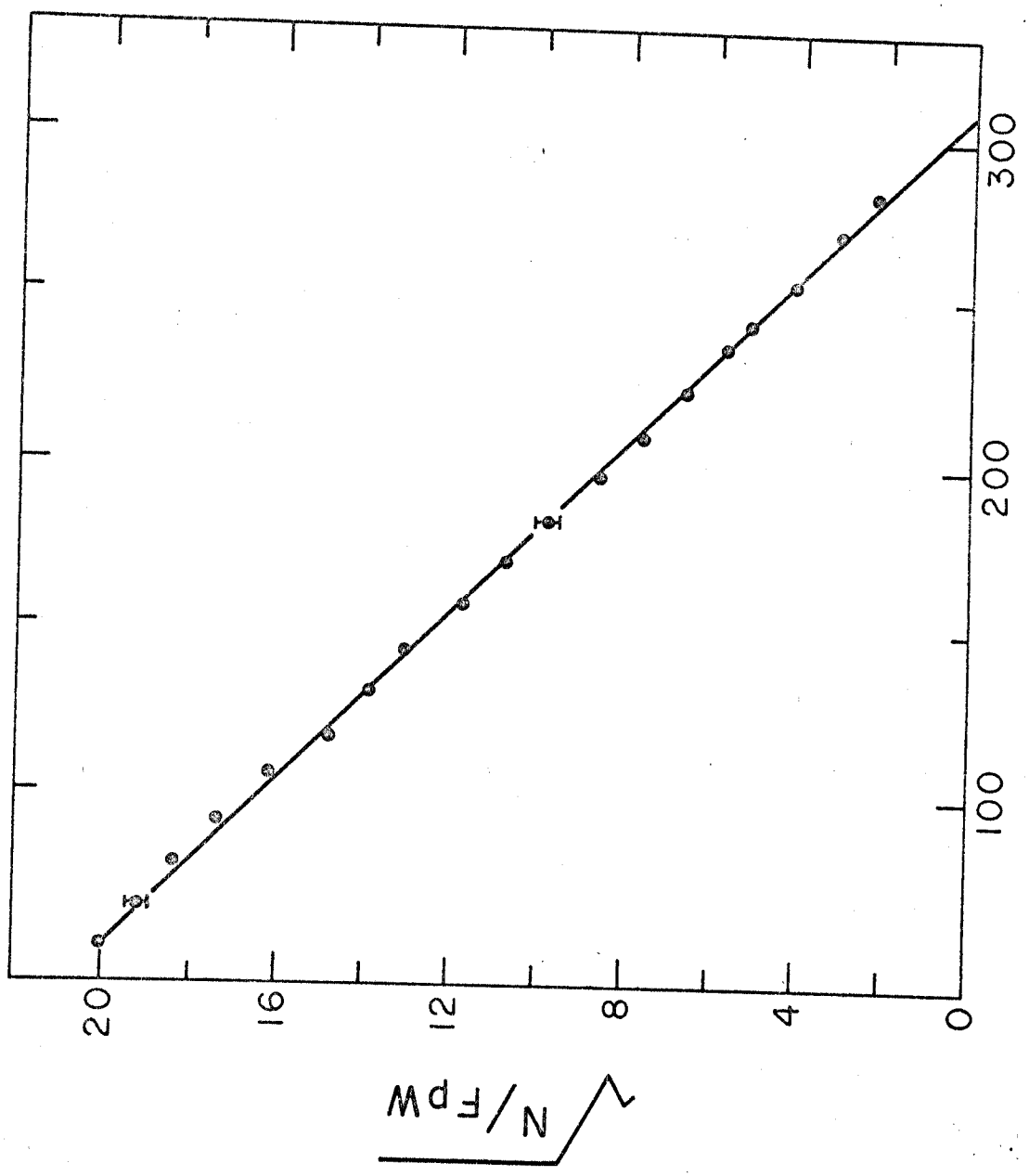

Figure 10. Fermi-Kurie plot of electron spectrum in coincidence with the 1089 keV gamma transition in ^{123}Sn.

with the 1420 keV end-point energy that has been reported for the ground state transition and the 1089 keV measured for the gamma ray energy.

In order to check the reliability of the scintillation spectrometer in reproducing the β-spectrum shape, the ^{123}Sn was replaced by a ^{60}Co source of comparable intensity and thickness. This source is very convenient in this case since it has an allowed β transition, with approximately the same end-point energy[29] (~ 314 keV) as ^{123}Sn. The β spectrum was recorded in coincidence with the 1173 keV gamma photopeak and a Fermi-Kurie plot of the spectrum was again found to be linear with an end point energy of 306 ± 15 keV. This is taken to indicate that the ^{123}Sn results are correct.

The relative intensities of the β transitions were determined from the ground state beta singles intensity and the 1089 keV gamma intensity using the known efficiency of the gamma detector[25] and assuming 100 percent efficiency for the β-detector. It was found that only 0.6 percent of the ^{123}Sn decays go to the 1089 keV state. From the gamma ray relative intensities given above, it was concluded that only 0.04 percent and 0.001 percent of the β-decays take place to the 1032 and 1187 keV levels, respectively. The log ft values[41] obtained from these intensities are 9.1, 10.5, 9.0 and 11.3 for transitions to the ground, 1032, 1089 and 1187 keV levels, respectively. These values suggest a first forbidden character for these β-transitions, which is consistent with the shape measurement on the

transition to the 1089 keV level.

4.B.iv. Discussion of Proposed Decay Scheme

The results described in the previous sections have been utilized to construct the decay scheme shown in Figure 11. The spin and parity assignments for the ^{123}Sn parent and ^{123}Sb ground states have been taken from previously reported measurements.[46] The assignment of a spin of 9/2 or 11/2 for the 1089 keV level is suggested by the allowed (or non-unique first forbidden) shape of the beta transition to this state and by the prompt decay to the ground state. The only evidence for assignment of spins 7/2 through 11/2 to the 1032 keV state is the log ft value for the beta transition to this state and the presence of a prompt ground state gamma transition. The spin of the 1187 keV state may be > 11/2, deduced from the absence of a ground state transition. However, no positive information is available on this level and therefore no assignment has been made. The parities of these states are suggested to be positive on the basis of log ft values.

Included in Figure 11, for comparison, is the decay scheme of the $11/2^-$ state of ^{121}Te. Both decays, as might be expected, are quite similar, both in the positions of the excited states of the corresponding antimony isotopes and in the log ft values for transitions to these states.

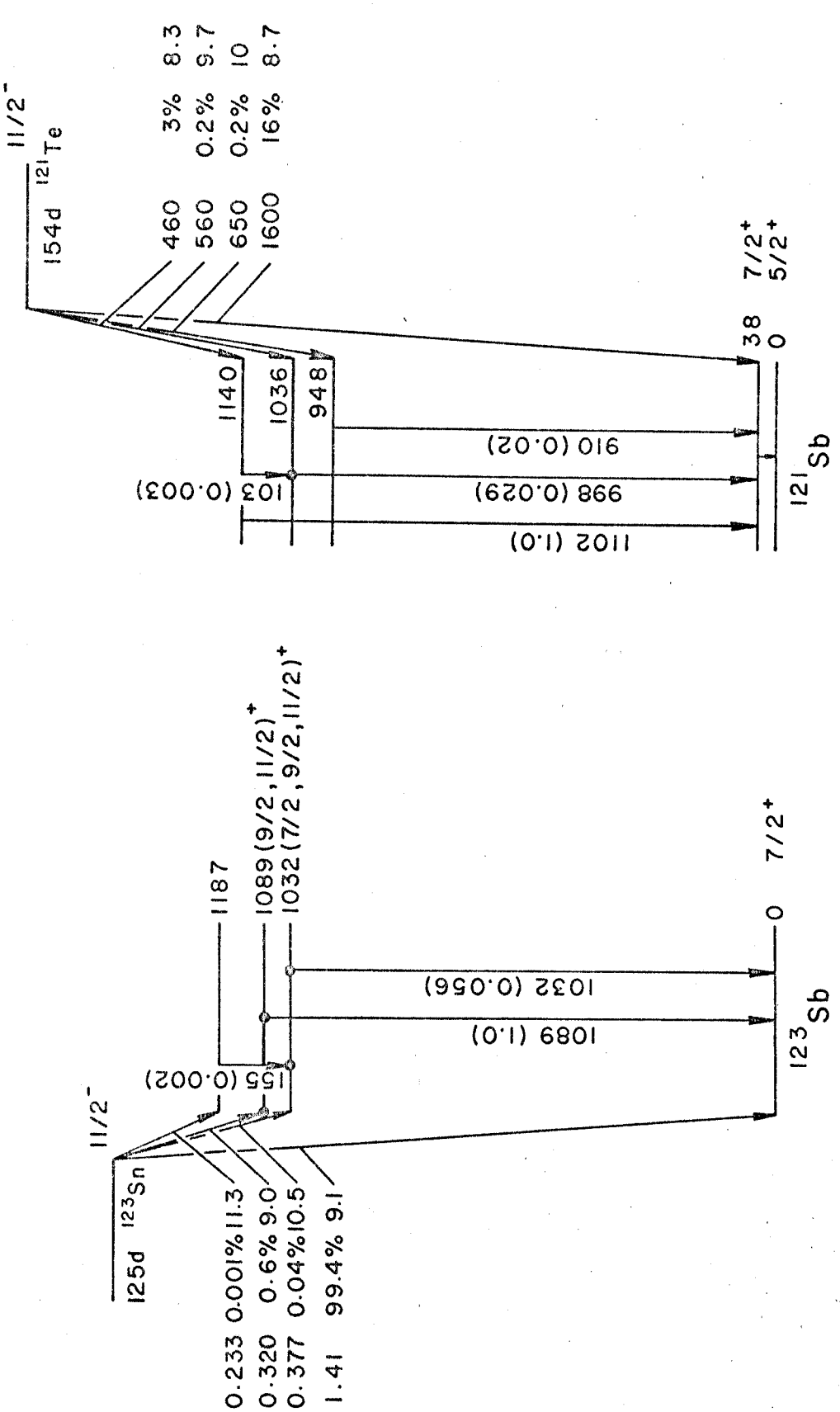

Figure 11. Proposed decay scheme of 125 day ^{123}Sn, compared with the decay scheme of ^{121m}Te.

4.C. The Decay of ^{125}Sn

4.C.i. The Gamma Ray Singles Spectrum

The spectrum was first studied using a NaI(Tl) detector. The results were essentially the same as those obtained by previous investigators[47] and therefore are not shown here. However, it soon became evident upon performing coincidence measurements using two NaI(Tl) detectors, which will be discussed later, that several of the peaks actually contained two or more photopeaks. These peaks had been previously ascribed to single gamma-ray transitions. In order to study the spectrum more carefully, a Ge(Li) detector was employed. The spectra from this detector were recorded on the 1024 channel analyzer in order to keep the energy per channel less than 2.5 keV. Many spectra were taken over a period of approximately four weeks to ensure that the peaks observed decayed with the correct half life. Several spectra were also taken with a 3 mm thick lead absorber to determine the effects of summing and no differences in the relative intensities of any of the peaks could be observed (after correcting for absorption). Figures 12 and 13, respectively, show the low and high energy portions of the spectrum. The spectrum shown in Figure 12 was taken approximately two weeks after the chemical separation and a number of peaks are observed which can be attributed to the growth of the ^{125}Sb daughter. The broad peak at $\sim$ 100 keV is due to backscatter of the 158.5 keV photons.

The energies of the peaks above 700 keV were determined by recording the ^{125}Sn spectrum simultaneously with a number of

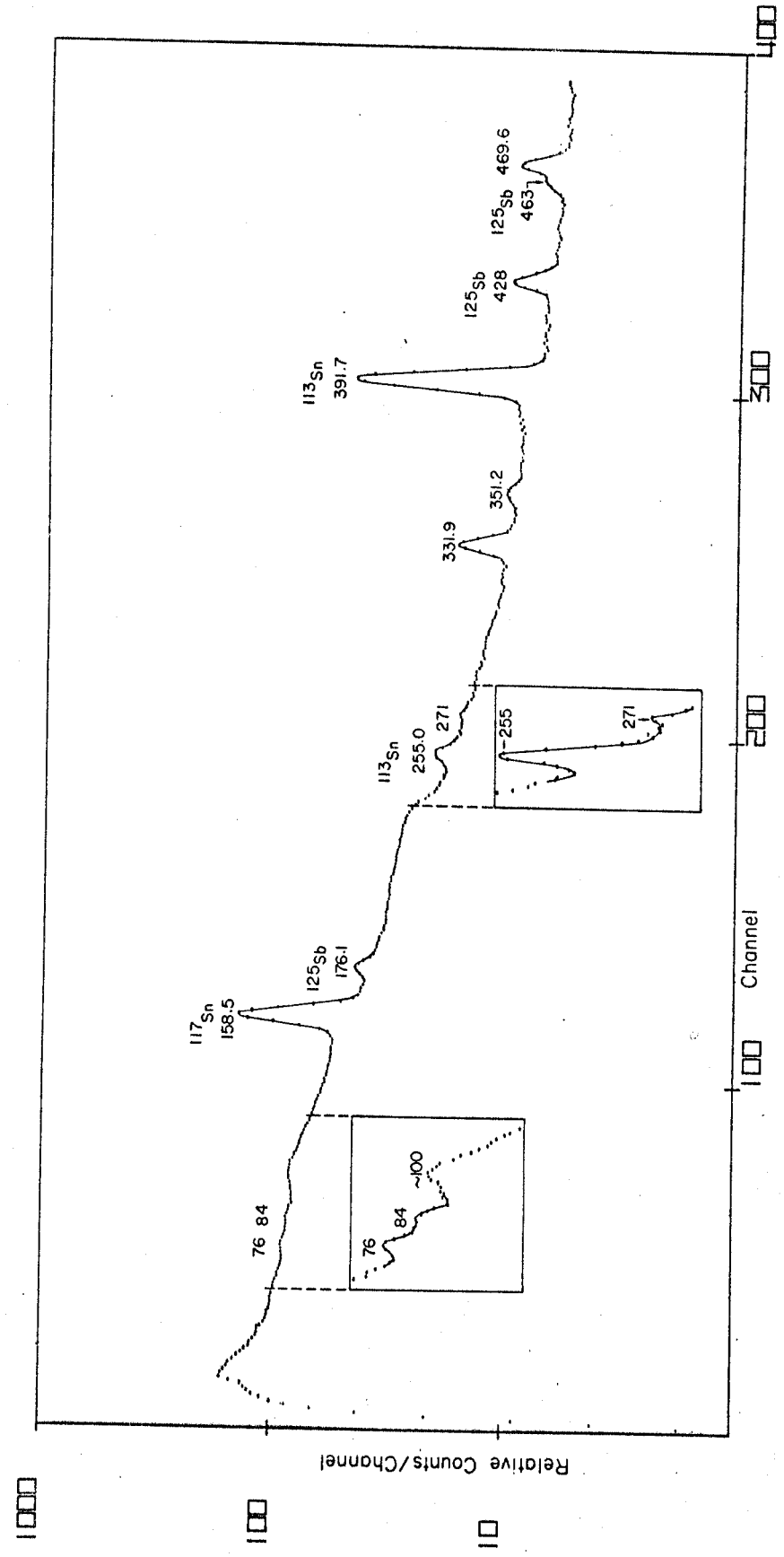

Figure 12. Ge(Li) spectrometer spectrum of low energy photons emitted in the decay of 9.7 day ^{125}Sn.

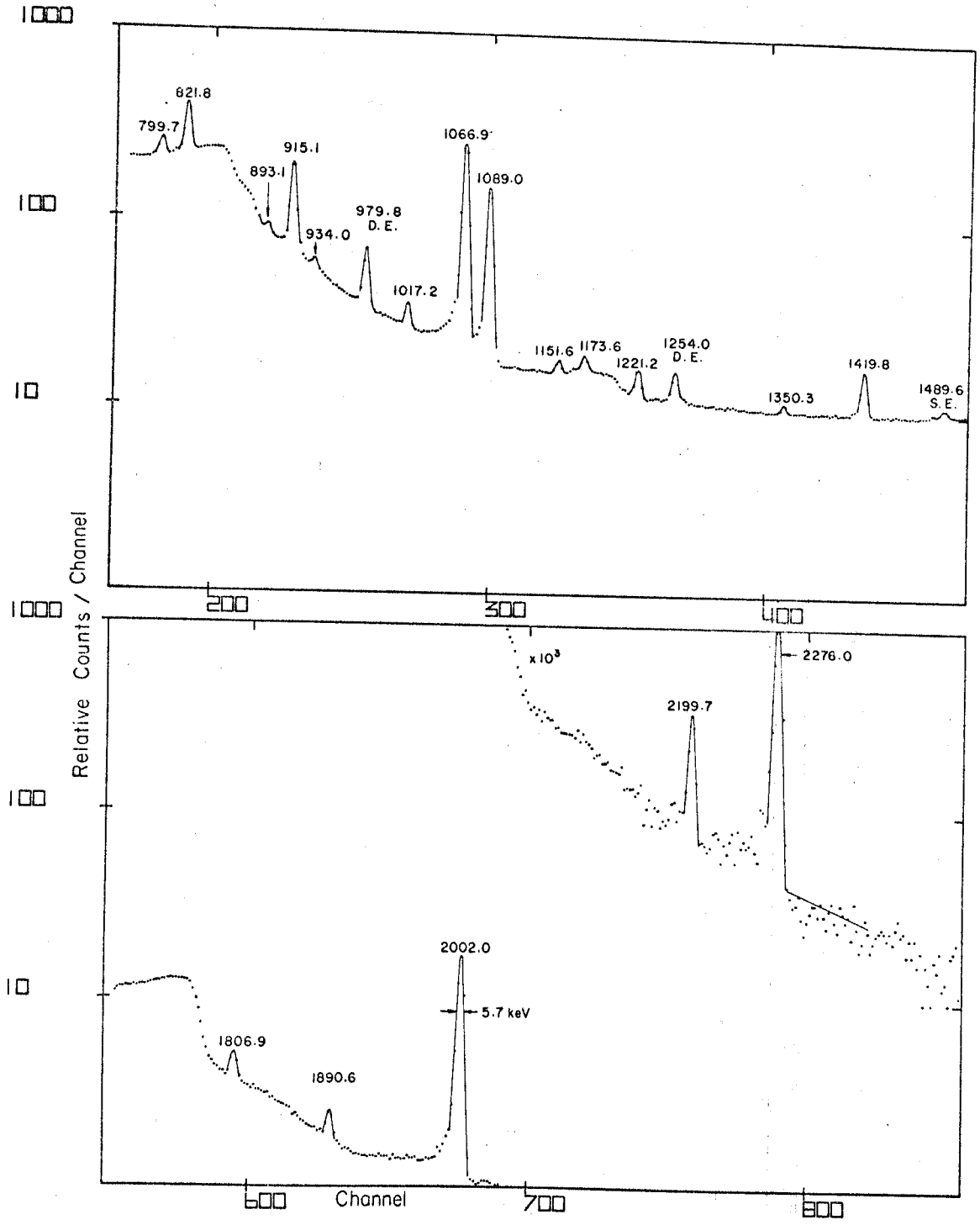

Figure 13. High energy gamma ray spectrum of 9.7 day ^{125}Sn taken with a 4mm x 2cm Ge(Li) detector.

standard sources having transitions with well known energies. These were: ^{22}Na (511.01 keV), ^{137}Cs (661.60 keV), ^{60}Co (1173.23 and 1332.48 keV) and ThC" (2614.47 keV plus the 1592.46 keV double escape peak).[48] In the low energy portion of the spectrum, the calibration points used were ^{152}Eu (121.8 and 344.3 keV),[49] ^{22}Na and ^{137}Cs. The peak positions were determined by subtracting an interpolated linear background from each peak and taking a weighted average of the channels in the peak. A least square fit of a quadratic calibration curve was then made to the calibration points. The energies obtained in this way were reproducible to within better than 1 keV.

The relative intensities of the ^{125}Sn peaks were determined by subtracting a linear background from each of the photopeaks to determine the total number of counts in the peak and utilizing the efficiency curve given in Chapter 3. The results of the energy and intensity measurements are summarized in Table 2.

4.C.ii. Gamma-Gamma Coincidence Studies

Extensive coincidence studies using two NaI(Tl) detectors have been made previously.[47] Similar experiments were performed in these studies and the multi-parameter feature of the 1024 channel analyzer utilized to study the shape and position of specific peaks in coincidence with various portions of the spectrum. This technique was used to show a definite downward shift in the "1075" keV peak, which consists primarily of the unresolved 1066.9 and 1089.0 keV photopeaks, when the gate was moved from the 332 or 470 keV peaks to the 822 or 915 keV peaks.

Table 2. Energy and intensity measurements on gamma rays emitted in the decay of ^{125}Sn using a Ge(Li) detector.

Energy (keV)[a]	Intensity	Energy (keV)	Intensity
76 ± 2	0.008 ± 0.004	1066.9	1.000
84 ± 2	0.009 ± 0.005	1089.0	0.641
271 ± 2	0.010	1151.6	0.012
331.9	0.166	1173.6	0.015[b]
351.2	0.030	1221.2	0.024
469.6	0.163	1350.3	0.0066
799.7	0.113	1419.8	0.064
821.8	0.468	1806.9	0.017
893.1	0.016	1890.6	0.0090
915.1	0.444	2002.0	0.288
934.0	0.020	2199.7	0.006
1017.2	0.029	2276.0	0.028

a) The energies, except where noted, were reproducible to within 1 keV and are believed to be accurate to at least 0.5 keV. The accuracy of the relative intensities of the strong transitions is limited by the accuracy of the efficiency curve, which is approximately 10 percent. The intensities of the weak transitions (< 0.05) are all within ± 20 percent except where noted.

b) Corrected for the unresolved double escape peak from 2199.7 keV photons by estimating the ratio of the double escape peak to photopeak from the values obtained for the 2002 and 2276 keV transitions which were 1.95 and 4.17, respectively.

This indicates that the 332 and 470 keV transitions are in coincidence with the 1089 keV transition while the 822 and 915 keV photons are in coincidence with the 1067 keV transition. In order to confirm these results, coincidences between the NaI(Tl) detector and the Ge(Li) detector were studied. The analyzer was gated on the 1067 and 1089 keV photopeaks in the Ge(Li) spectrum separately. The spectra observed by the NaI(Tl) detector in coincidence with the 1089 and 1067 keV photopeaks are shown in Figures 14 (a) and 14 (b), respectively. These spectra have been corrected for chance coincidences using the automatic chance correction feature of the multichannel analyzer (Chapter 3). In addition to bearing out the conclusions made above, these spectra show that there are still transitions in the 820 and 915 keV regions which are in coincidence with the 1089 keV transition. Also observable in part (a) is a peak at 1150 keV and in part (b) there is a very broad peak in the 1170-1220 keV region.

In order to better determine which transitions are in coincidence with the 1067 and 1089 keV transitions, a Ge(Li) spectrum was taken gating the analyzer on the combined 1067-1089 keV photopeaks in the NaI(Tl) counter. The result, shown in Figure 15, indicates that the following gamma rays are in coincidence with one, or possibly both, of the 1067 and 1089 keV transitions: 272, 332, 351, 470, 800, 822, 893, 915, 934, 1153, 1173, 1221 keV.

Using the two NaI(Tl) detectors for higher efficiency, coincidences between the 332 and 470 keV transitions and photons above 1000 keV were studied and the results are shown in Figure 16. Part (a) of Figure 16 shows the spectrum in coincidence with the

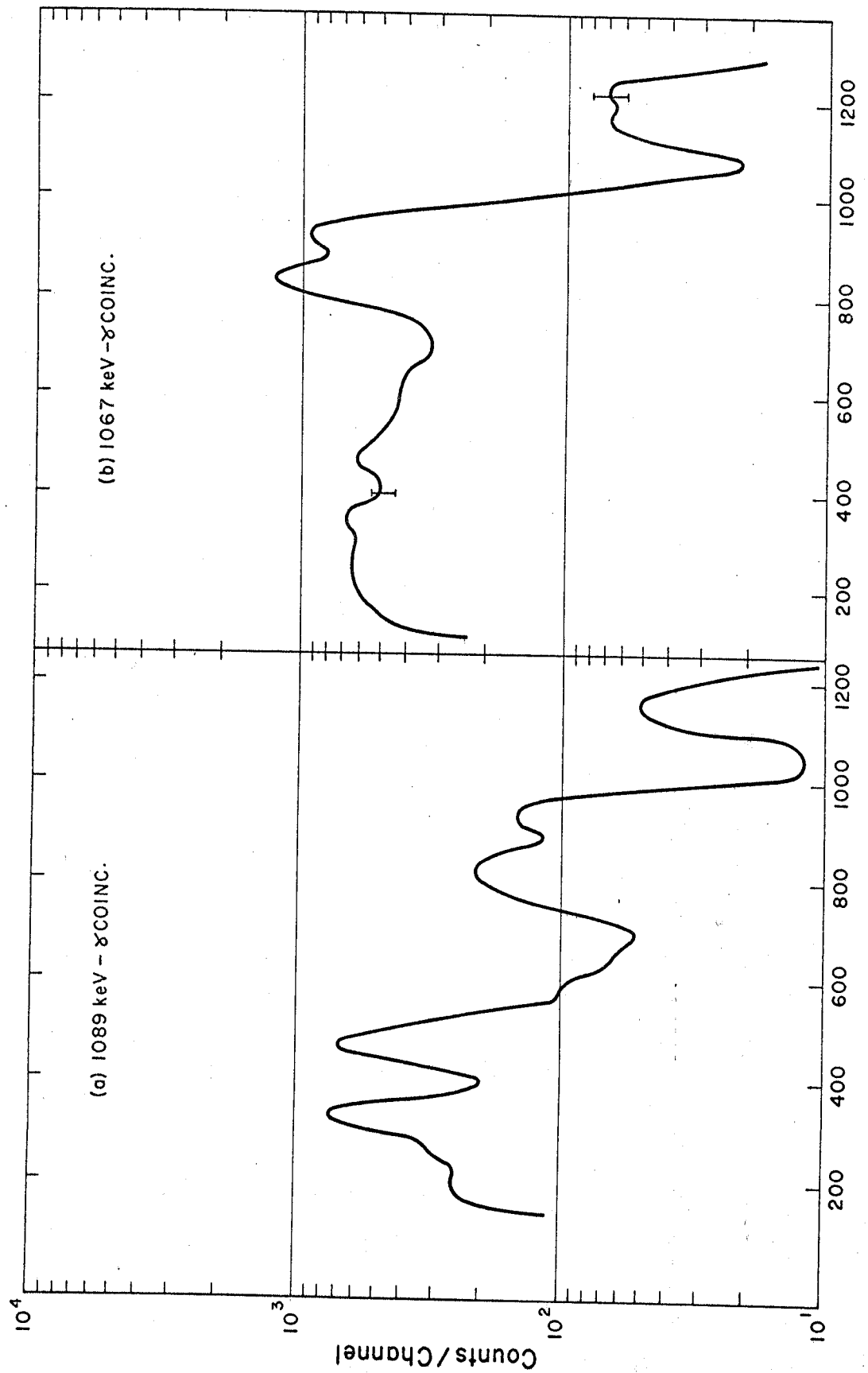

Figure 14. Spectra observed with a NaI(Tl) detector in coincidence with (a) 1089 and (b) 1067 keV transitions as seen by a Ge(Li) detector; ^{125}Sn.

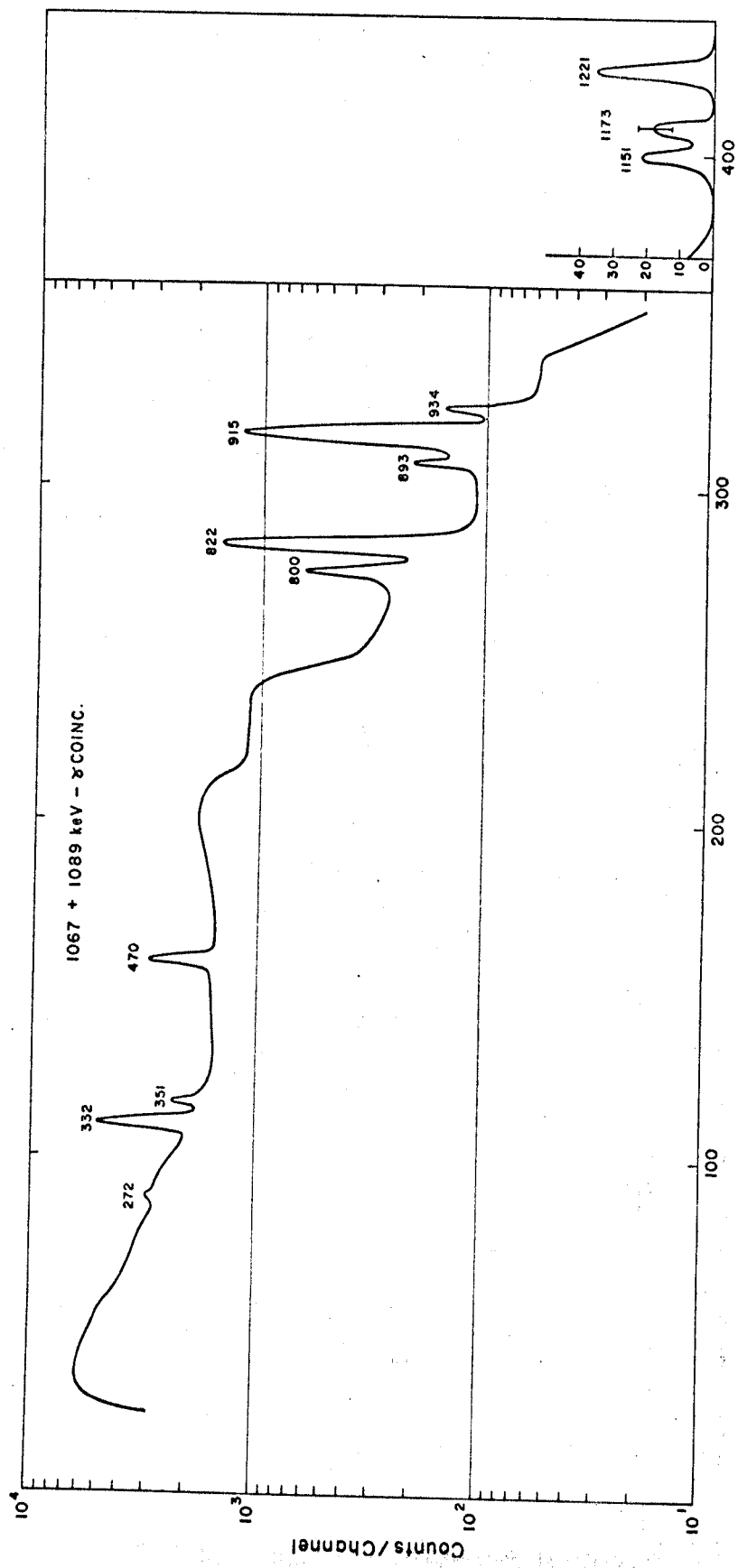

Figure 15. Ge(Li) spectrum of ^{125}Sn in coincidence with the unresolved 1067 and 1089 keV photopeaks detected with a NaI(Tl) crystal.

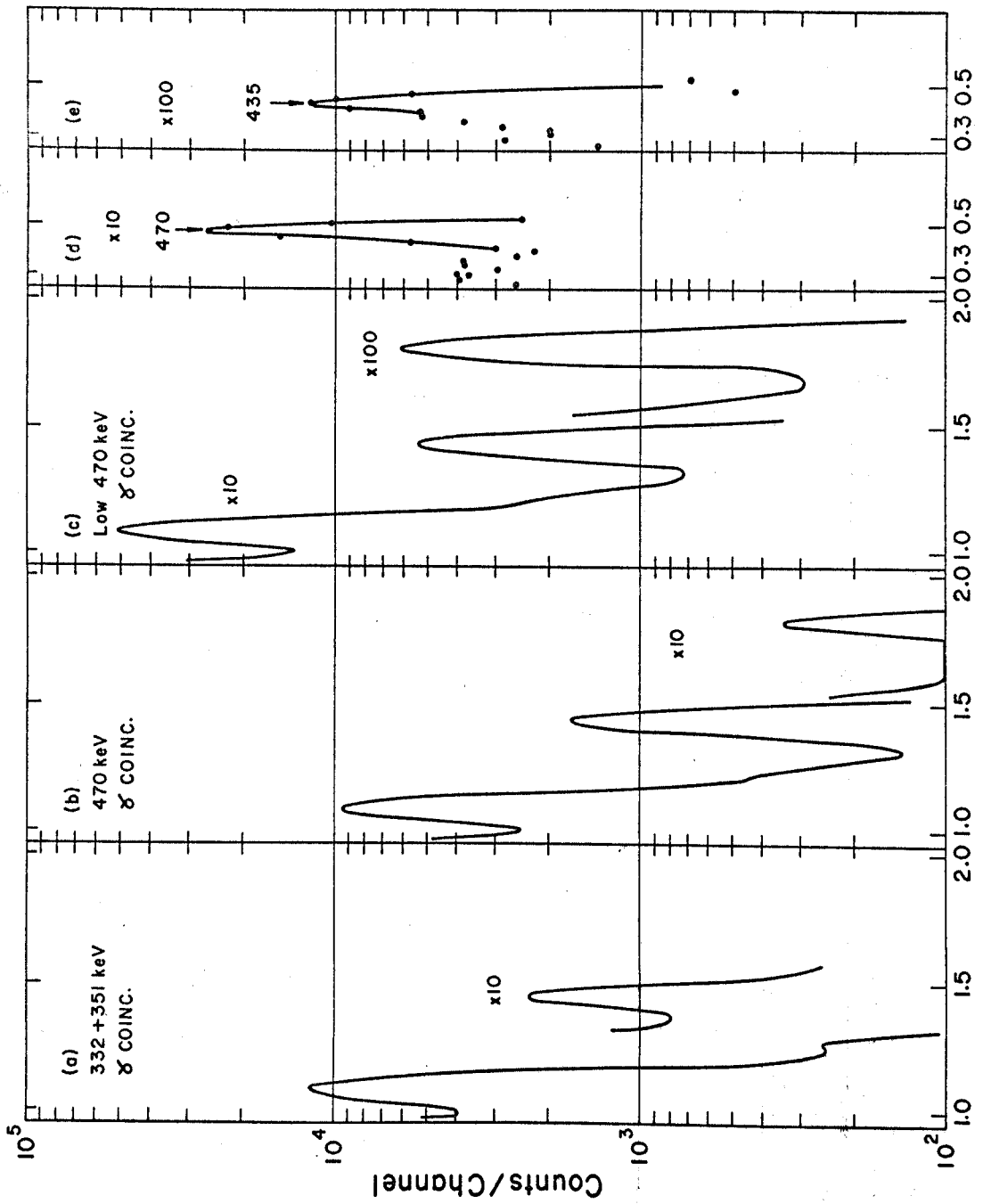

Figure 16. Gamma spectra in coincidence with the (a) 332 plus 351, (b) 470, (c) low side of the 470, (d) 1420 and (e) 1806 keV energy regions.

unresolved 332 and 351 keV transitions. Chance corrections were made as mentioned above. Corrections for underlying Compton distributions were made by subtracting coincidences obtained with regions slightly above and below the peak being studied. This coincidence spectrum shows that, even after these corrections, a weak coincidence between the 1420 and either 332 or 351 keV transition still remains. Part (b) of Figure 16 shows the spectrum in coincidence with the 470 keV photopeak. Here it can be seen that, in addition to the previously observed 470-1089 and 470-1420 keV coincidences, there is a very weak line at approximately 1800 keV. In order to study this coincidence more thoroughly, the gate was moved to the low energy side of the 470 keV photopeak, giving the spectrum shown in Figure 16(c). Here the ratio of the height of the 1800 keV peak to that of the 1420 keV peak is obviously enhanced over that of part (b), indicating that the transition in coincidence with the 1800 keV photons has an energy slightly less than 470 keV. In order to confirm this conclusion, the analyzer was gated on the 1420 and 1800 keV regions separately, giving the spectra shown in parts (d) and (e), respectively, of Figure 16. Here it was observed that, whereas the peak in coincidence with the 1420 keV transition came at 470 keV, the peak observed in coincidence with the 1800 keV region was shifted down to 435 keV. This coincidence, which had not been reported previously, is in good agreement with the appearance of the 1806 keV peak in the singles spectrum. The fact that a 435 keV peak is not observed in the Ge(Li) singles spectrum is not surprising since the intensity of this transition was found to be only

approximately 50 percent of the intensity of the very weak 1806 keV line. With this intensity, the peak height would have been much less than the statistical fluctuations in the 435 keV region of the Ge(Li) spectrum.

Multi-parameter coincidences with the 272, 332 and 470 keV regions with photons between 700 and 1200 keV were also studied using two NaI(Tl) detectors. Spectra obtained in coincidences with these regions are shown in Figures 17 (a), (b) and (c), respectively. The weak coincidences of the 272 keV transition with the 915 and 1075 keV regions have not been reported previously. The fact that the 1075 keV region is somewhat enhanced over that of the 915 may indicate an incomplete subtraction of the coincidences with the partially unresolved 332 keV peak. However, the absence of an 822 keV peak, within statistics, indicates that the correction for the underlying Compton distribution was reasonably accurate.

The spectrum obtained in coincidence with the 332 keV peak is shown in part (b) of Figure 17. It was found that, in addition to the previously observed 1089 keV coincidence, peaks at 822 and 1017 keV were also evident. Again, corrections for coincidences with the strong underlying Compton distributions have been made and the absence of a 915 keV peak shows that the correction was accurate. Unfortunately, the 332 and 351 keV peaks are unresolved so the peaks in the 822 and 1017 keV regions may be in coincidence with either or both of these transitions. The 820 and 1017 keV peaks are reduced by a factor of approximately 5 over the 1089 keV peak, indicating that only a fraction of the 332 plus

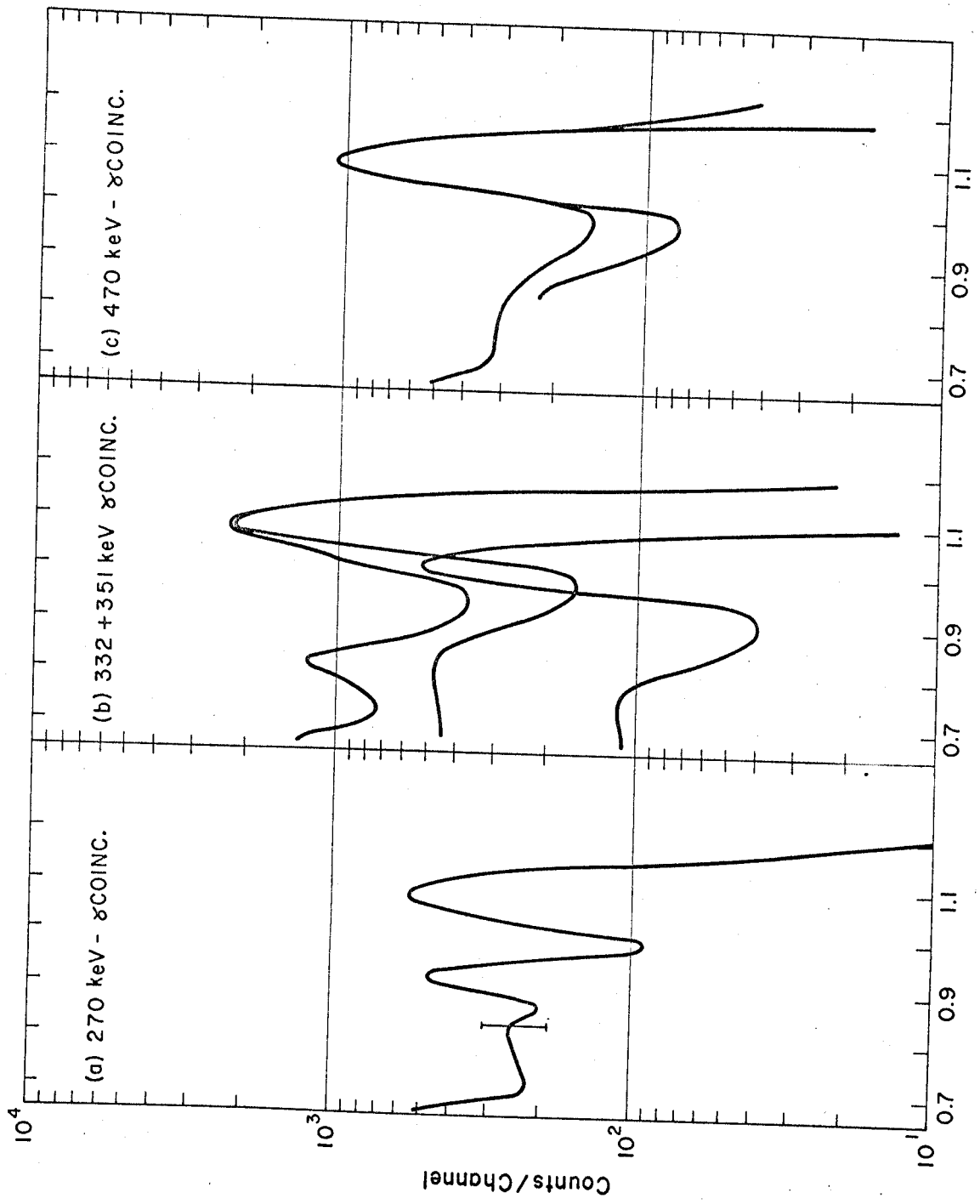

Figure 17. Coincidence spectra obtained by gating on the (a) 272, (b) 332 plus 351 and (c) the 470 keV regions of the ^{125}Sn gamma spectrum.

351 keV photons are in coincidence with these transitions.

The coincidences obtained by gating on the 470 keV peak, shown in part (c) of Figure 17, are identical to the results obtained in previous studies, and shows only the strong 1089 keV peak. The enhancement seen in the Compton valley is due to the Compton distribution of the 1420 keV photons.

4.C.iii. Beta-Gamma Coincidence Studies

Several studies of beta-gamma coincidence relations have been made to help confirm the location of a number of transitions in the decay scheme. The beta detector geometry utilized an external source, as discussed in Chapter 3, while a NaI(Tl) crystal was used to detect the photons. The observed end-point energies of beta rays in coincidence with the 332, 470, 822, 915 and 1089 keV photons were: (450 plus 940), (450), (420, (350) and (1300 plus 500) keV, respectively. Due to the inaccuracy of the calibration curve, obtained by using Compton edges of known gamma rays, an error of $\sim$50 keV is assigned to each of these end-point energies. The end-point energy obtained from the beta singles spectrum for the ground state transition was 2360 $\pm$ 50 keV. These values are in good agreement with previous measurements.[47]

4.C.iv. Construction of a Proposed Decay Scheme

The decay scheme constructed on the basis of these studies is shown in Figure 18. Many features are quite similar to those proposed previously.[47] The location of the states at 1089.0, 1890.6 and 1982.0 keV are fixed by the beta-gamma coincidence data obtained both in this and other studies. In addition, beta-gamma

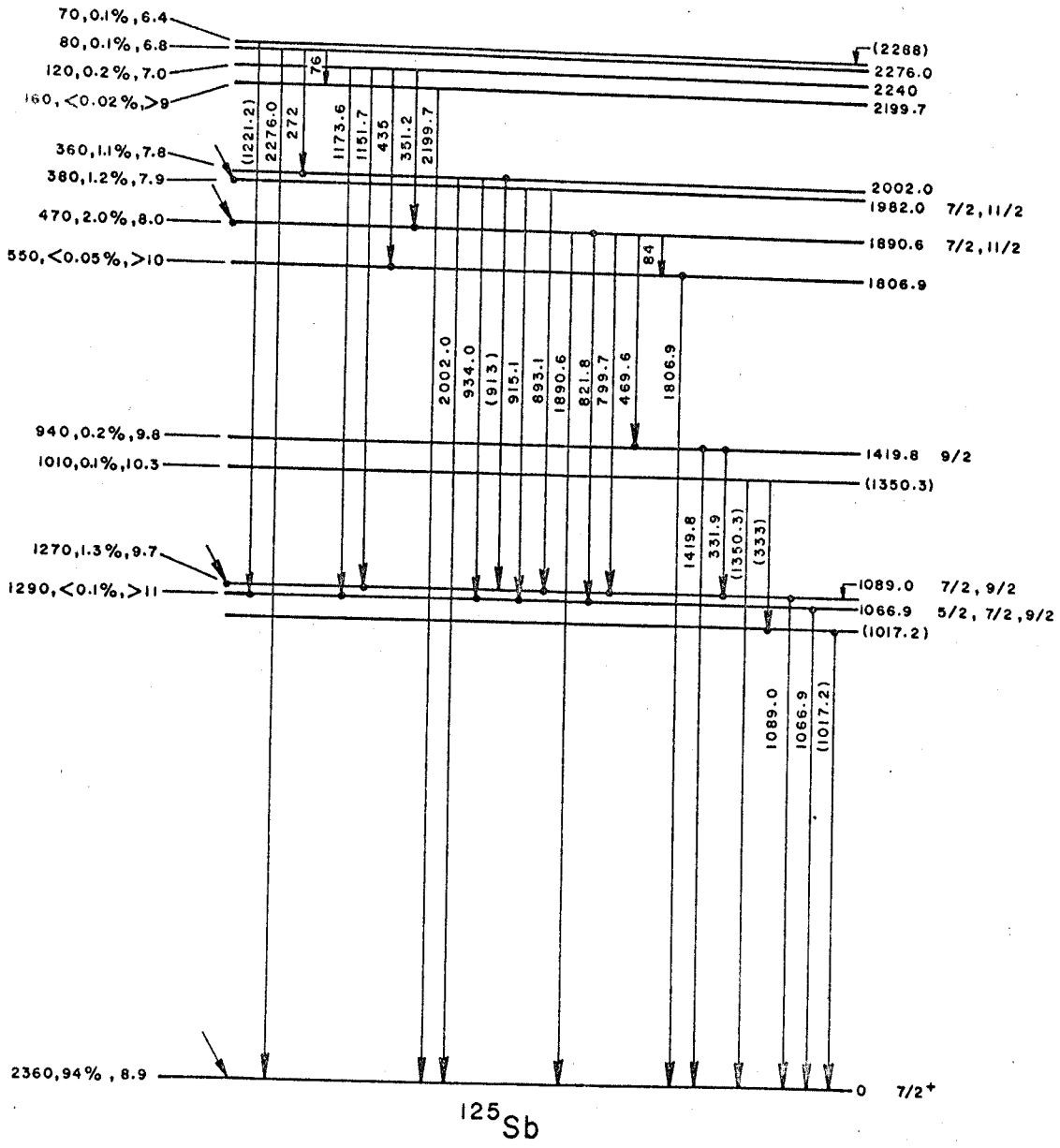

^{125}Sb

Figure 18. Proposed energy level scheme for ^{125}Sb as seen in the decay of 9.7 day ^{125}Sn.

coincidences with the 2002.0 and 1419.8 keV transitions have been reported and determine the position of these transitions.

Since no gamma-gamma coincidences could be observed with the 2276, 2200, 1890 or 1350 keV transitions, these probably go to the ground state. The high intensity of the 1067 keV gamma indicates that it also is a ground state transition.

The assignment of levels at 1017 and 1350 keV, which is only tentative, is based on the observation of the 1017 keV transition in coincidence with the 332 keV region and assumes that a 333 keV transition, which would be unresolved in the Ge(Li) spectrum, exists between these states. The presence of such a transition is also indicated by the fact that the energy difference between the 1419.8 and 1089.0 keV levels is 1.1 keV less than the 331.9 keV obtained for the transition between these levels. This is believed to be outside the precision of the present measurements. (It seems unlikely that the proposed 333 keV transition is the same as the transition from the first excited state of ^{125}Sb seen in the decay of the 9 min activity of ^{125}Sn. This has been reported to be 326 keV.[47] The latter value should be accurate to better than 4-5 keV while the separation of the 1017 and 1350 keV peaks obtained here is accurate to better than 1 keV.)

The level at 2240 keV is suggested by the 1151-1089 and 1173-1067 keV gamma-gamma coincidences. The enhancement of the 822 keV region in coincidence with the 330 keV region can also be explained by assuming that the 351 keV transition connects the 2240 and 1890 keV levels, thus adding additional evidence for the 2240 keV state.

A level at 2288 keV has been proposed to explain the existence of the 1221 keV transition in coincidence with the 1066.9 plus 1089.0 keV photopeaks. The 1221 keV transition is believed to proceed to the 1067 keV state since a very broad peak is produced in the 1173-1221 keV region when gating on the 1066.9 keV photons. This is compared to the much narrower peak obtained in this region when the gate is set on the 1089 keV photopeak.

A 913 keV transition connecting the 2002.0 and 1089.0 keV levels has been proposed to explain the existence of the 1089-915 keV coincidence, which was found to be much too strong to be due solely to the weak, unresolved 893 keV transition. Such a transition can be expected since the 934 keV transition to the 1066.9 keV state was observed and it appears, from the angular correlation studies to be described later, that the 1066.9 and 1089.0 keV levels may have similar spins. This assignment is also supported by the fact that the intensity of the 915 keV peak, relative to that of the 822 keV peak, is reduced by approximately 10 percent in coincidence with the 1066.9 keV transition. In addition, such a transition can explain the existence of the 272-915 keV coincidences.

The 76 and 84 keV transitions are placed between the 2276 and 2199.7 keV states and the 1890.6 and 1806.9 keV states, respectively, on the basis of energy differences.

One rather large discrepancy still exists in the energy measurements. The 821.8-1066.9 and 799.7-1089.0 keV cascades both add up to 1888.7 keV, whereas the energy measured for the transition which is assumed to proceed to the ground state is

1890.6 keV. This may indicate that additional levels exist near 1890 keV. One possible test would be the detection of 351-1890 keV coincidences. Unfortunately, this coincidence is extremely weak and no conclusions concerning its existence could be made in this study.

Also shown on the decay scheme are the log ft values[41] for beta transitions to the various levels in ^{125}Sb. The relative beta intensities were determined from the beta singles and beta-gamma coincidence spectra in conjunction with the gamma ray intensities. These log ft values suggest that the transitions are probably first forbidden, which, in conjunction with an $11/2^-$ assignment for 9.7 day ^{125}Sn, suggests positive parity for the states in ^{125}Sb which are populated in the beta decay of 9.7 day ^{125}Sn.

4.C.v. Angular Correlation Measurements

The angular correlations between all of the prominent gamma ray cascades were measured using two NaI(Tl) detectors and the coincidence circuitry discussed in Chapter 2. The detectors were enclosed in anti-scattering shields and care was taken to keep the source-detector geometry such that the detection solid angle was defined by the NaI(Tl) crystal and not by the opening in the lead cone of the shield. Coincidences were recorded on the multiparameter analyzer in 45° steps from 90° to 270°. In this manner the analyzer could generally be used to measure several correlations simultaneously. Equivalent chance coincidences were subtracted automatically and corrections for underlying Compton

distributions were obtained from coincidences with regions above and below the photopeak being studied. The results, after correction for source decay and finite detector size, are given in Table 3.

Many of these correlation functions are limited in accuracy by the presence of unresolved transitions or by intense Compton distributions. For example, the 332-1089 and 470-1089 keV correlations had to be corrected for the Compton distributions due to the 822 and 915 keV photons arising from coincidences with the unresolved 1067 keV photopeak. These corrections were made using the technique mentioned above. Similar corrections were necessary for the 332-470 keV coincidences due to the presence of the 1067 and 1089 keV transitions. Even more serious than the Compton corrections is the existence of unresolved photopeaks as is the case for both the 332-1089 and the 822-1067 keV correlations. The 332-1089 keV coincidences contain approximately an 18 percent contribution from the 351-1067, 1089 cascades while the 800-1089 keV cascade contributes approximately 20 percent to the 822-1067 keV correlation data. Uncertainties introduced by these unresolved transitions in the A_2 coefficient of the desired correlation function were estimated by assuming a function of the form $1 + A_2P_2(\cos\theta)$, with $|A| \leq 0.2$, for the unresolved cascade. This appears to be a reasonable assumption in view of the magnitude of the correlation coefficients obtained for other cascades in this nucleus. The coefficients and errors given in Table 3 for the 332-1089 and 822-1067 keV cascades include the corrections thus deduced for these correlation functions. No corrections were made for the A_4

Table 3. Summary of angular correlation measurements on photons from ^{125}Sb.

Cascade	A_2	A_4	A_2 [a]	A_4 [a]
469.6- 331.9	-0.060±0.029	+0.024±0.031	-0.045±0.012	+0.005±0.014
469.6-1089.0	-0.099±0.034	-0.020±0.040		
469.6-1419.8	+0.072±0.020	+0.029±0.028		
331.9-1089.0	-0.070±0.050	+0.020±0.040	-0.030±0.020	-0.010±0.021
821.8-1066.9	+0.180±0.050	+0.020±0.040	+0.123±0.013	+0.012±0.015
915.1-1066.9	+0.130±0.009	+0.028±0.011	+0.125±0.013	+0.003±0.015
1151.6-1089.0 plus 1173.6-1066.9	+0.151±0.031	-0.031±0.039		

[a] These values are given by Devare and Devare.[50]

coefficients since the experimental values are very small; therefore, these values are not to be considered very reliable. The 470-1420 and 915-1066.9 keV cascades are relatively free from interfering radiations and no such corrections were made. The 915 keV peak does contain a small contribution from the 893 and 934 keV transitions (and a possible 913 keV transition proposed above) but the net contribution is less than 10 percent and should have little effect on the measured correlation function.

No attempt was made to analyze the 1151-1089 and 1173-1067 keV correlation data since the two are completely unresolved and have approximately the same intensity.

Also included in Table 3, for comparison, are several coefficients obtained by Devare and Devare.[50] The values obtained for the 470-332 and 915-1067 keV cascades are in good agreement; those for the 332-1089 and 822-1067 keV correlations are in better agreement if comparison is made with the coefficients obtained in this before correcting for unresolved peaks. These were $1 - (0.046 \pm 0.029)P_2(\cos\theta) + (0.014 \pm 0.036)\, P_4\, (\cos\theta)$ and $1 + (0.157 \pm 0.010)P_2(\cos\theta) + (0.02 \pm 0.02)P_4(\cos\theta)$ for the 332-1089 and 822-1067 keV cascades, respectively.

The large uncertainties introduced by these corrections make it impossible to find a unique set of spin assignments for the nuclear levels and mixing ratios for the transitions between them. In an effort to gain some insight into the nature of the transitions, the following spin assignments, obtained in previous studies,[47,50] have been assumed. The ground state and 1089 keV excited state have been assigned spin-parity $7/2^+$ on the basis of

beta spectrum shape measurements and arguments presented above concerning the measured log ft values. The beta transition to the 1420 keV state has also been studied[50] and the results indicate that the transition has a statistical shape, suggesting that the transition is either allowed or non-unique first forbidden.[45] The log ft value is in agreement with the latter assignment which suggests a $9/2^+$ or $11/2^+$ spin-parity assignment for the 1420 keV state (higher values being ruled out by the strong ground state transition).

Under these restrictions, the 11/2 assignment for the 1420 keV state can be ruled out on the basis of the 470-332 keV and the 470-1420 keV correlation functions since, for this assignment, the two functions would be identical (assuming negligible octupole contributions). The possible spins for the 1890 keV state were limited to 7/2, 9/2 or 11/2 since there is a beta branch (probably first forbidden) to this state. This limits the possible spins to 7/2 through 15/2, and a transition to the 7/2 ground state, which suggests spins assignments 3/2 through 11/2. Only the 7/2 and 11/2 values were found to be consistent with the angular correlation data.

The two remaining spin sequences for the 1890, 1420, 1089 and ground states, 7/2-9/2-7/2-7/2 and 11/2-9/2-7/2-7/2, were analyzed using the double mixture curves of Arns and Weidenbeck.[31] The results for the first sequence suggest quadrupole mixtures of 0 to 12 percent (-), 99.5 to 100 percent (-), 6 to 12 percent (-), and 99.5 to 100 percent (-) for the 1089, 332, 470 and 1420 keV transitions, respectively. In the second case, the respective

mixtures are 4 to 10 percent (-), 99.7 to 100 percent (-), 15 to 34 percent (+) and 99.5 to 100 percent (-). The signs in parentheses refer to the signs of δ, the mixing amplitudes, with the sign for the 332 keV transition being for the case where it is the first transition in a cascade. This sign must be reversed[51] when analyzing the 470-332 keV correlation.

Analyses of the 822-1067 and 915-1067 keV cascades were attempted but only a limited amount of information could be deduced. Possible spin assignments for the states involved were limited by the following arguments: the 1982 keV state could be limited to 7/2 through 15/2 by the existence of a first forbidden (from the log ft value) beta transition to this level while the values for the 1890 keV state were limited to 7/2 and 11/2 by the analysis of the 470-332 and 470-1420 keV correlation functions given above. The possible assignments for the 1067 keV state were limited to 3/2 through 11/2 in view of the prompt decay to the ground state. With these restrictions, it was found that the only spin assignments consistent with the 915-1067 keV correlation function were 7/2 or 11/2 for the 1982 keV state and 5/2, 7/2 or 9/2 for the 1067 keV level. The latter values are also consistent with the 822-1067 keV correlation function. The quadrupole mixtures in the 822, 915 and 1067 keV transitions could not be determined since nearly all values were found to agree with the correlation data.

4.D. The Decay of ^{127}Te and ^{127m}Te

4.D.i. Gamma Ray Spectrum of ^{127}Te Isomers

The γ ray spectrum of the ^{127}Te source is shown in Figure 19. The top curve shows the spectrum obtained with a NaI(Tl) crystal having approximately 8.5 percent resolution for the 0.662 MeV line from ^{137}Cs. The bottom curve shows the spectrum obtained using a Ge(Li) detector. Singles spectra were recorded over a 5 month period and it was found that the peaks at 458, 694 and 728 keV decayed with a half life of approximately 30d and are believed to be due to ^{129}Te. By comparing spectra, it was found that the 572 keV line is due to a strong transition in ^{121}Te and that the 159 keV line is due to ^{123}Te.[32] The remainder of the peaks are due to ^{127}Te. Of particular interest are the two at 591 and 657 keV. Only the latter transition had been previously observed.[52] The lower energy transitions have all been previously observed, although the 203 and 214 keV peaks had not been resolved. The relative intensities of the gamma rays due to ^{127}Te are given in Table 4. The 145 keV peak is not observed in the singles spectrum due to its low intensity. However, its presence has been established in previous studies[52] and in coincidence studies discussed below.

4.D.ii. Coincidence Studies

Coincidence measurements were made using two NaI(Tl) crystals. These detectors were separated by 90° and enclosed in lead shields to reduce the effects of crystal to crystal Compton scattering. Copper absorbers 0.25 mm thick were placed on the

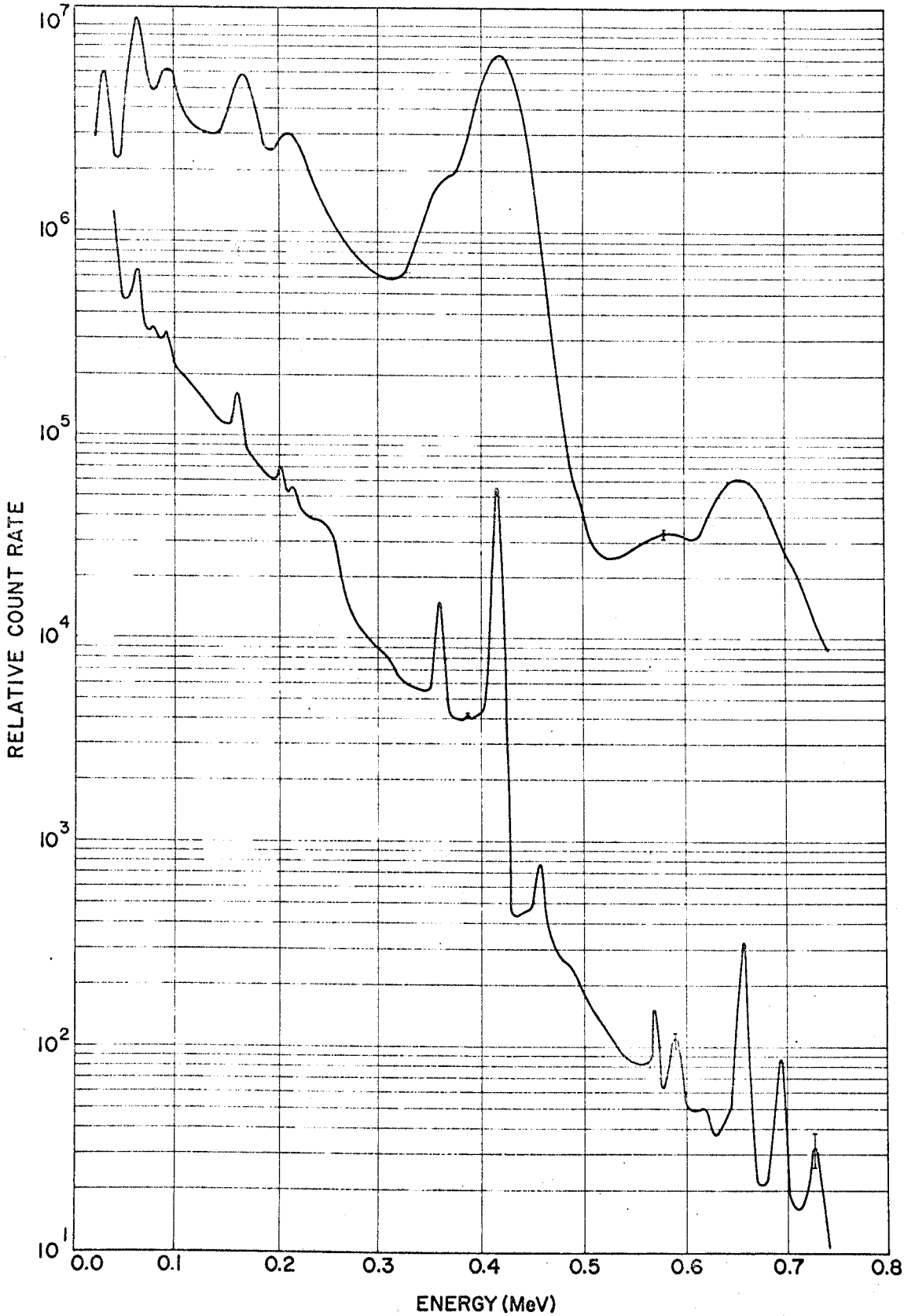

Figure 19. Gamma ray spectra of ^{127}Te taken with a (upper curve) 7.6cm x 7.6cm NaI(Tl) crystal and (lower curve) a 4mm x 2cm Ge(Li) detector.

Table 4. Summary of data on photons emitted in the decay of ^{127}Te.

Transition Energy (MeV)[a]	Relative Photon Intensity[a]	Transition Rates[b]	Coincident Transitions (MeV)
0.0576±0.0005	61±1	0.89	0.145, 0.214 0.360, 0.591 0.657
0.087±0.001(I.T.)	25±1	99.2	
0.145±0.005[c]	0.51±0.06[c]	0.0023	0.0576, 0.214
0.203±0.001	5.4±0.2	0.018	0.214
0.214±0.001	3.9±0.2	0.013	0.0576, 0.145 0.203
0.360±0.0005	14.8±0.1	0.0465	0.0576
0.417±0.0005	100	0.313	
0.591±0.001	0.22±0.04	0.00062	0.0576
0.657±0.001	1.43±0.06	0.00434	0.0576

[a] These data, with the exception of the 0.145 MeV transition data, were obtained from the Ge(Li) runs.

[b] Number of transitions, photons plus conversion electrons, per 100 disintegrations of ^{127m}Te. Corrections for internal conversion were made using the conversion coefficients calculated by Rose[40] assuming the lowest multipole order for the transitions consistent with the proposed decay scheme.

[c] Energy and intensity obtained from coincidences with the 0.214 MeV transition.

faces of the crystals to reduce the intensity of the strong K-X-ray.

The coincidence spectra obtained between the 0 to 100 keV and 70 to 720 keV regions are shown in Figure 20. The data were recorded on the multi-parameter analyzer operating in the 64 channel by 16 channel mode. Part (a) shows the spectrum seen by the first detector in coincidence with 57.6 keV photons entering the second detector. The 591, as well as the previously observed 360 and 657 keV transitions can be seen. These results suggest the presence of excited states at 417, 649 and 715 keV. The 145 and 214 keV lines, expected on the basis of previous measurements,[52] are too weak to be observed above the Compton distribution of the strong 360, 591 and 657 keV photopeaks. Similarly, parts (b), (c) and (d) are spectra seen by the second detector in coincidence with the 360, 591 and 657 keV photons seen by the first detector, respectively. Parts (c) and (d) have not been corrected for the overlap of the 591 and 657 keV photopeaks. They serve only to indicate that there is no appreciable broadening of the 57.6 keV peak in coincidence with the 591 keV region as would be expected if there were a transition connecting the 715 and 649 keV states.

The spectrum in coincidence with the unresolved 203 and 214 keV transitions is shown in Figure 21. This spectrum has been corrected for chance coincidences but not for coincidences with the underlying Compton distribution. Any such correction would have limited accuracy since the 203-214 keV peak lies so close to the Compton edge of the 360 keV Compton distribution. Coincidences

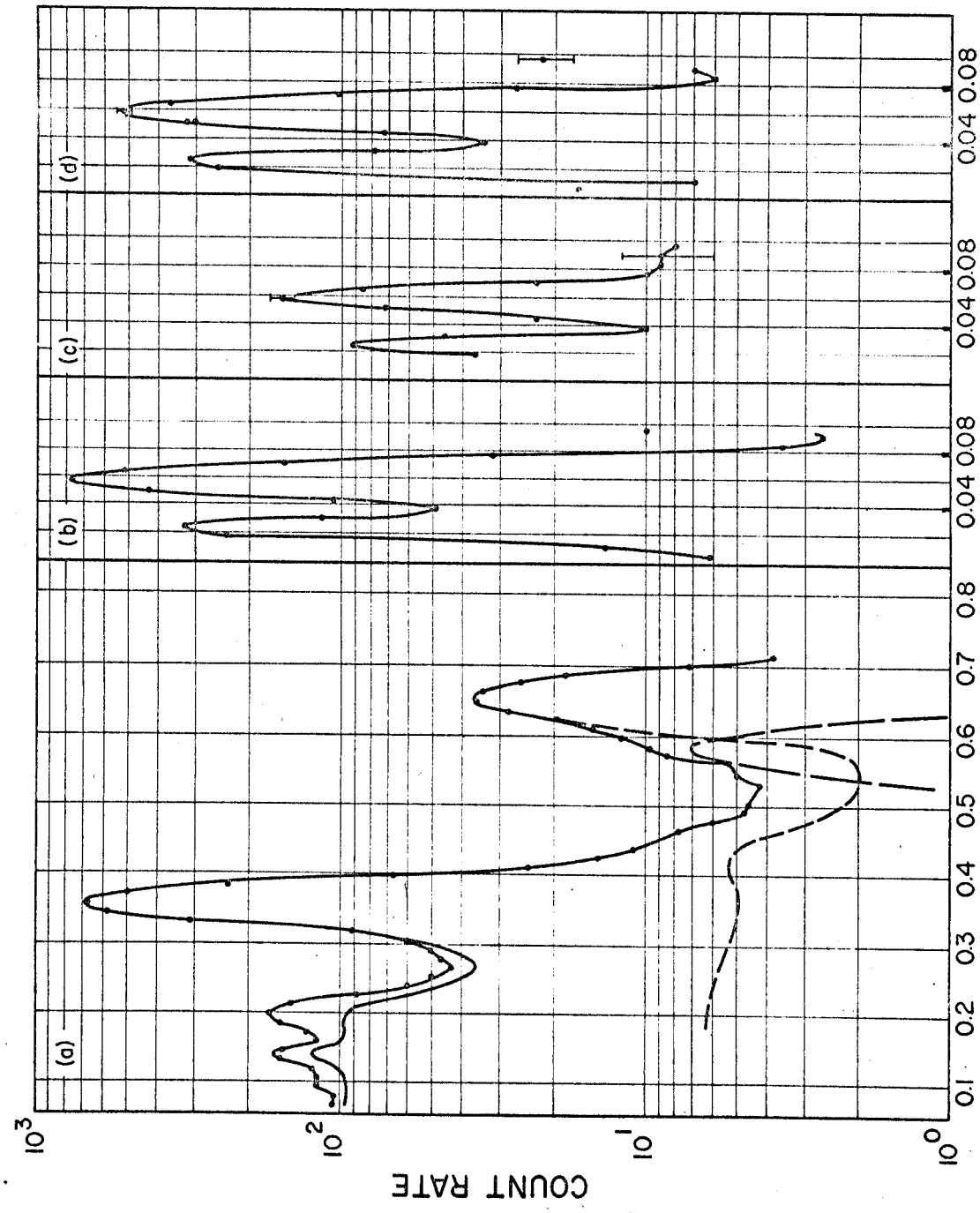

Figure 20. Spectra of ^{127}Te taken in coincidence with (a) 57.6, (b) 360, (c) 591 and (d) 657 keV photons.

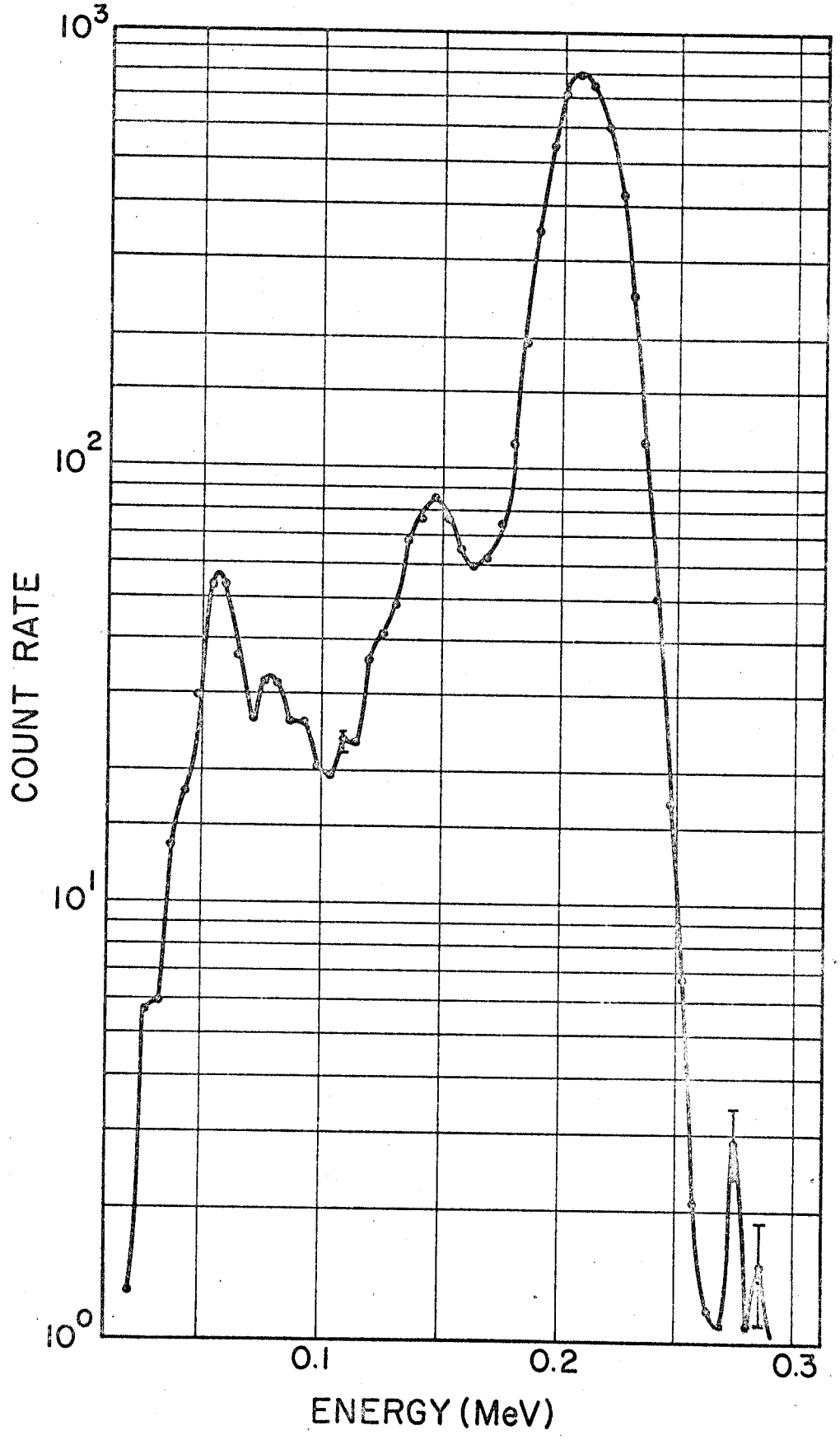

Figure 21. Coincidence spectrum obtained by gating on the unresolved 203-214 keV photopeaks in the ^{127}Te spectrum.

were recorded at both 90° and 180° and an average of the two sets of data used to obtain the approximate relative intensity of the 145 keV transition. The 57.6 keV peak is also visible, but an accurate intensity measurement could not be made due to the large contribution from the Compton distribution of the 360 keV transition. The peak at approximately 86 keV is due primarily to backscatter of the 203 and 214 keV gamma rays. These results suggest that ^{127}Te and ^{127m}Te decay to excited states at 57.6, 203, 417, 649 and 715 keV in ^{127}I.

4.D.iii. ^{127}Te Angular Correlation Measurements

Angular correlation measurements were made using the same experimental apparatus as in the coincidence studies. The multiparameter feature of the multichannel analyzer was again utilized in correcting for underlying Compton distributions. Coincidences were recorded at angles of 90, 135, 180, 225, and 270 degrees between detectors and corrections made for source decay and source asymmetry. The resulting correlation function coefficients were corrected for finite detector size.[26] The results are given in Table 5. The source used to obtain the coefficients for the cascades involving the 57.6 keV transition had to be kept very dilute since it was observed that the anisotropy of these correlations was strongly dependent on the source density. A semi-quantitative study of the effect of source density was made by adding or evaporating conc. HCL to change the volume of the source. The volumes used ranged from approximately 0.02 cm^3 to 0.1 cm^3 and contained approximately 5 mg of source material. The measured

Table 5. Summary of angular correlation measurements on ^{127}Te photons.

Cascade Gamma 1-Gamma 2	A_2	A_4	Spin Sequence	Mixing Amplitude (Gamma 1)[a]
0.214-0.203	+0.224±0.005	-0.005±0.005	5/2-3/2-5/2	+0.20±0.02 or > 200
0.360-0.0576	+0.32±0.02	0.00±0.02	5/2-7/2-5/2	-0.18±0.08 or -2.29 ±0.07
0.591-0.0576	+0.27±0.06	+0.15±0.15	7/2-7/2-5/2	-1.7±0.3
			9/2-7/2-5/2	+0.24±0.13 or +5.68±0.09
0.657-0.0576	-0.078±0.037	-0.033±0.089	7/2-7/2-5/2	-0.33±0.08 or +2.14±0.08
			9/2-7/2-5/2	-0.24±0.07 or -3.00±0.01
			11/2-7/2-5/2	

[a] Mixing amplitudes of +0.52±0.05 and -0.0803±0.0063 for the 0.203 and 0.0576 MeV transitions, respectively, were given by Geiger[53] and utilized in analyzing these angular correlation data.

anisotropy varied from 0.33 ± 0.08 for the smallest volumes used to 0.58 ± 0.08 for the largest volumes. The larger value is believed to be approximately the unperturbed value since the anisotropy was essentially constant for the more dilute sources employed. The possibility that this effect is due to increased small angle Compton scattering at the higher source densities was investigated by placing a 3 mm thick aluminum absorber around the dilute source. No attenuation of the anisotropy in this and other similar experiments was observed. The attenuation of angular correlation anisotropies in liquid sources is believed to be due to the interaction between the electric quadrupole moment of the nucleus in its intermediate state and electric field gradients existing at the nucleus.[54] These gradients may be expected in radioactive nuclei since, in the beta-decay process, the nucleus acquires a net positive charge which leads to a rearrangement of the atomic electron structure. The 57.6 keV state of ^{127}I may be susceptible to such an interaction since it has both a large quadrupole moment[55] and a relatively long lifetime.[53] The effect of the interaction will be dependent upon the length of time during which the nucleus exists in its intermediate state. It is expected that the atomic rearrangement process would occur very quickly. The degree of attenuation of the anisotropy is, therefore, somewhat surprising. By measuring the anisotropy as a function of the delay between the two radiations, one may be able to determine the magnitude of the interaction more directly. An attempt was made by W. Chaffee[56] to make this measurement on the 360-57.6 keV cascade in ^{127}I. Unfortunately, in order to obtain

useful results the resolving time of the apparatus must be much shorter than the lifetime of the nuclear state. The apparatus available did not have this capability and no positive results could be obtained.

The 214-203 correlation did not show any attenuation effects. This result is expected on the basis of the short lifetime of the intermediate state (as measured by Geiger[53]).

In analyzing the results of the angular correlation experiments, spin assignments 5/2, 7/2 and 3/2 were used for the ground states and the 57.6 and 203 keV excited states, respectively.[53] In addition, the E2 admixtures 0.64 ± 0.10 percent and 21 ± 3 percent obtained by Geiger[53] for the 57.6 and 203 keV transitions, respectively, were used. With these restrictions, it was found that, while the 214-203 keV correlation is consistent with 1/2, 3/2 or 5/2 for the spin of the 417 keV state, the 360-57.6 keV correlation, obtained with a dilute source, was consistent with only the 5/2 assignment. These results require that the mixing amplitude δ(E2/M1) of the 203 keV transition be positive. The 214 keV transition is required to be either 4.4 ± 0.7 percent or > 99.9 percent E2 (assuming positive parity for the 417 keV state as indicated by the log ft values given below) with (E2/M1) positive in the first case and either positive or negative in the second case. The 360-57.6 keV correlation also required that the mixing amplitude for the 57.6 keV transition be negative and that the 360 keV transition be either (3.1 ± 1.4) percent or (84 ± 3) percent E2 (again assuming positive parity of the 417 keV state) with the mixing amplitude negative in both cases. Unfortunately,

very little can be concluded from the 657-57.6 keV correlation since it is consistent with 5/2, 7/2, 9/2 or 11/2 for the 715 keV state spin. Similarly, the 591-57.6 keV correlation is consistent with the 5/2, 7/2 or 9/2 assignment for the 649 keV state.

A summary of the spin sequences and mixing amplitudes suggested by the angular correlation measurements is included in Table 5. The 5/2 spin assignments for the initial state in the 657-57.6 and 591-57.6 keV cascades, although consistent with the angular correlation results, can be excluded on the basis of log ft values as discussed in sec. 4.D.iv.

An attempt was made to measure the 214-145 keV anisotropy but the strong 214-203 MeV peak made such a measurement impractical.

4.D.iv. Summary of ^{127}Te Results

The decay scheme of ^{127}Te suggested by these studies is shown in Figure 22 and is similar to that previously proposed[52,53] with the addition of a β branch from ^{127m}Te to the 649 keV state of ^{127}I. The angular correlation measurements, in conjunction with previously published conversion electron data,[53] allow unique spin assignments for the first three ^{127}I excited states populated by ^{127}Te β decay. They also limit the possible spin assignments for the 649 and 715 keV states.

Log ft values,[41] obtained using β energies and intensities deduced from γ-ray energies and intensities, suggest that the transitions from ^{127m}Te to the 57.6, 649 and 715 keV states of ^{127}I are probably first forbidden. This suggests a spin

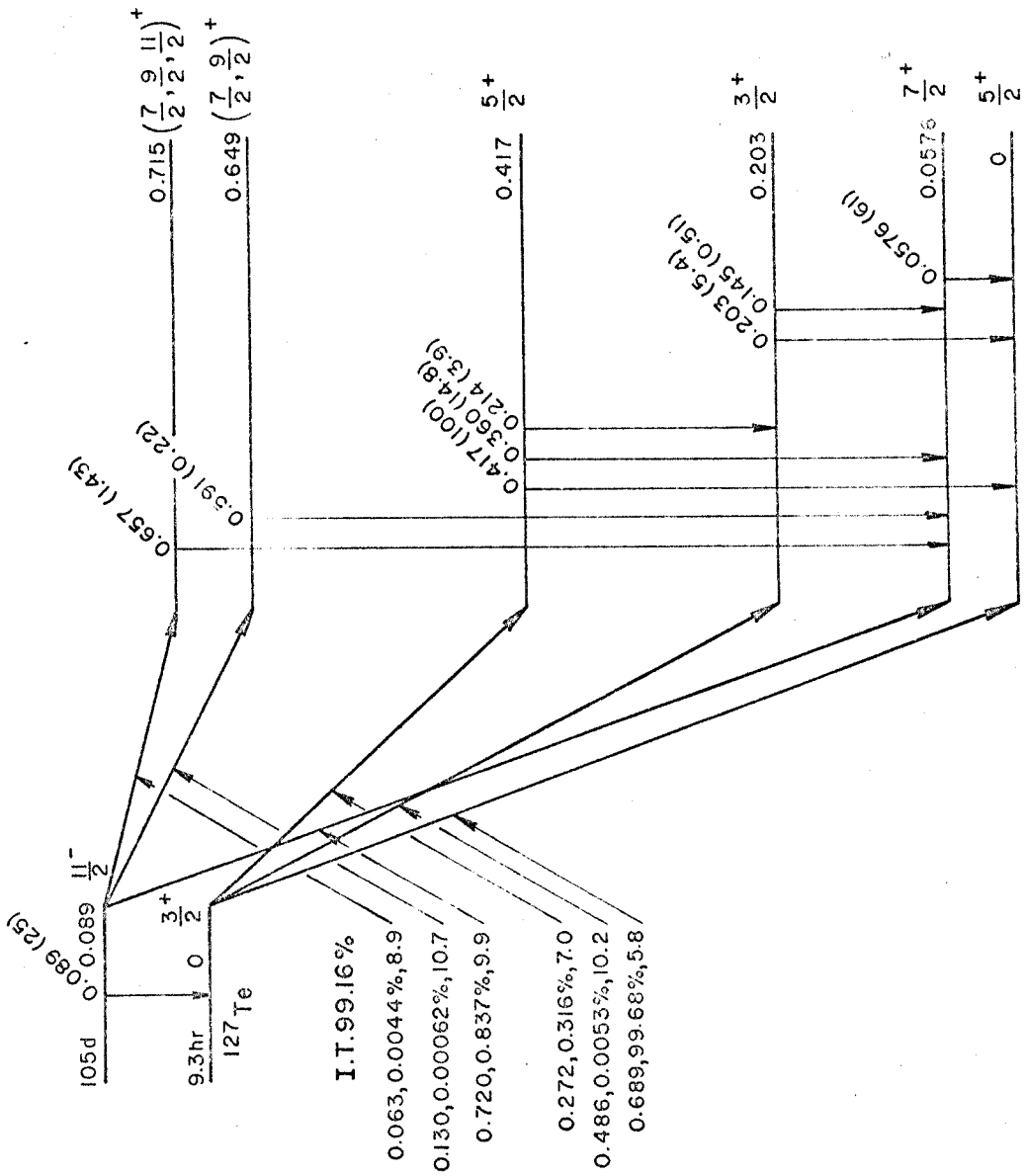

Figure 22. Proposed decay scheme of ^{127}Te and ^{127m}Te.

assignment of 7/2, 9/2 or 11/2 and positive parity for these states. This is consistent with the angular correlation results. The log ft values obtained for the decay of the ^{127}Te ground state suggests that the transitions to the ground and 417 keV states are allowed which would require a 1/2, 3/2, or 5/2 spin assignment and positive parity for these states, in agreement with the $5/2^+$ assignments made to these states on the basis of other data.[53]

CHAPTER 5

DISCUSSION OF EXPERIMENTAL RESULTS AND COMPARISONS WITH THEORY

With the exception of the ground or first excited, $7/2^+$, state, the energy levels of the nuclei studied here can be divided into two groups: a) those populated by the low spin ($1/2^+$ or $3/2^+$) isomer of the parent nucleus, and b) those excited in the decay of the $11/2^-$ state of the parent. The discussion of the states will be divided accordingly. Those in group a) will be confined to the low energy region ($\leq$ 600 keV), because first, only such states could be studied here, and second, relatively little data are available on the higher energy states populated by the low spin isomers.

5.A. The Low Energy States

In addition to the work reported here, several other experimental studies on the low-lying states of ^{121}Sb and ^{127}I have been made recently (see secs. 4.A. and 4.D.) and much of the data now available are summarized in Tables 6, 7 and 8. Table 6 lists some of the information available on the states themselves while Tables 7 and 8 are concerned with the M1 and E2 transition rates between these levels. The dipole moments (μ) and quadrupole moments (Q) given in Table 6 are compared with the single proton values (μ_{sp} and Q_{sp})[57] and the values obtained by Kisslinger and Sorenson[20] (μ_{KS} and Q_{KS}) using pairing-plus-quadrupole residual forces. The agreement between the experimental and the latter predicted values of the quadrupole moments is obvious.

Table 6. Properties of low energy states of ^{121}Sb and ^{127}I.

Energy State (keV)	Spin	Shell Model Assignment	Mean-life (seconds)	Electric Quadrupole Moment (barns)			Magnetic Dipole Moment (nuclear magnetons)		
				Q_{exp}	Q_{sp}	Q_{KS} (e)	μ_{exp}	μ_{sp} (d)	μ_{KS} (e)
				^{121}Sb					
0	5/2	$2d_{5/2}$		-0.29 (c)	-0.07 (d)	-0.43 (e)	3.359 (c)	4.8	2.24
37	7/2	$1g_{7/2}$	5.1×10^{-9} (a)			-0.44 (e)			
506	3/2	$2d_{3/2}$	2.7×10^{-12} (b)						
572	1/2	$3s_{1/2}$	1.2×10^{-11} (b)						
				^{127}I					
0	5/2	$2d_{5/2}$		-0.79 (c)	-0.07 (d)	-0.99 (e)	2.808 (c)	4.8	2.60
57.6	7/2	$1g_{7/2}$	2.68×10^{-9} (f)	-0.71 (g)	-0.08 (d)	-1.08 (d)	1.96 (k)		
203	3/2	$2d_{3/2}$	$<.55\times10^{-9}$ (f)						
			0.75×10^{-9} (h)						
375 (i)	1/2	$3s_{1/2}$							
418	5/2		4.6×10^{-12} (j)						

a) Y. Y. Chu, et al., Phys. Rev. 133 (1964) B1361 (delayed coincidences)

Table 6 (continued)

[b] F. R. Metzger and H. Langhoff, Phys. Rev. 132 (1963) 1753 (nuclear resonance fluorescence)

[c] G. H. Fuller and V. W. Cohen, Nuclear Moments, Appendix 1 to Nuclear Data Sheets (May, 1965)

[d] The single particle (proton) estimates were computed using the expressions given by de-Shalit and Talmi:[5]

Quadrupole moment $Q_{sp} = -\frac{2j-1}{2(j+1)}\langle r^2\rangle = -11.7 \times \frac{2j-1}{2(j+1)}\ fm^2$

Dipole moment (Schmidt values) $\mu_{sp} = \ell g_\ell + 1/2\ g_s$ for $j = \ell + 1/2$

$= \frac{j}{j+1}[(\ell+1)g_\ell - 1/2\ g_s]$ for $j = \ell - 1/2$

where, for an odd proton, $g_\ell = 1$, $g_s = 5.5855$ and for an odd neutron $g_\ell = 0$, $g_s = -3.8256$ (in nuclear magnetons)

[e] L. S. Kisslinger and R. A. Sorensen, Revs. Mod. Phys., 35 (1963) 853

[f] J. S. Geiger, Physics Letters, 7 (1963) 48 (delayed coincidences)

[g] G. J. Perlow and S. L. Ruby, Phys. Lett., 13 (1964) 198 (Mossbauer effect)

[h] R. H. Davis, A. S. Divatia, D. A. Lind and R. D. Moffat, Phys. Rev. 103 (1956) 1801 (Coulomb excitation)

[i] Not populated in the present studies. This state is populated in the electron capture decay of ^{127}Xe.

[j] H. Langhoff, Nuclear Physics 63 (1965) 425 (nuclear resonance fluorescence)

[k] P. N. Tandon, S. H. Devare and H. G. Devare, Congres International de Physique Nucleair, Paris (1964) (rotation of angular correlation in external magnetic field)

Table 7. Transition rates between low energy states of ^{121}Sb.

Transition Energy (keV)	Initial-Final State	Mean-life for gamma ray emission(sec)	Mixing ratio (or δ where known)	$B(E2)/(2j_f+1)$ exp.	$B(E2)/(2j_f+1)$ single proton	$B(E2)/(2j_f+1)$ KS[a]	M1 retardation $B(M1)_{theory}/B(M1)_{exp}$ S.P.	M1 retardation $B(M1)_{theory}/B(M1)_{exp}$ KS[a]
37	$1g_{7/2}-2d_{5/2}$	6×10^{-8}(b)	5×10^{-4}(b)	0.17	0.003	0.168	135	1/6
66	$3s_{1/2}-2d_{3/2}$	2.4×10^{-9}(c)	0.17 ± 0.03	20	0.057	0.134	31	1.3
469	$2d_{3/2}-1g_{7/2}$	3×10^{-11}(c)		1.04	0.035	0.98		
506	$2d_{3/2}-2d_{5/2}$	3×10^{-12}(c)	0.29 ± 0.09	1.1	0.008	0.141		
572	$3s_{1/2}-2d_{5/2}$	1.2×10^{-11}(c)		1.7	0.057	1.42		

a) L. S. Kisslinger and R. A. Sorensen, Revs. Mod. Phys. 35 (1963) 853

b) Y. Y. Chu, O. C. Kistner, A. C. Li, S. Monaro and M. L. Perlman, Phys. Rev. 133 (1964) B1361 (L subshell conversion electron ratios for multipolarity, delayed coincidence measurements for mean-life)

c) F. R. Metzger and H. Langhoff, Phys. Rev. 132 (1963) 1753, (nuclear resonance fluorescence)

Table 8. Transition rates between low energy states of ^{127}I.

Transition Energy (keV)	Initial-Final States	Mean-life gamma ray (seconds)	Mixing amplitude (δ)	$B(E2)/(2j_f+1)\times10^{50}e^2cm^4$			M1 retardation $B(M1)_{theory}/B(M1)_{exp}$	
				exp.	single proton	KS[a]	S.P.	KS[c]
57.6	$1g_{7/2}$-$2d_{5/2}$	8.1×10^{-9}[b]	-0.08[b]	1.2	0.003	0.04	66	5
145	$2d_{3/2}$-$1g_{7/2}$	$\leq6\times10^{-9}$[b]		≥2.7[b] 1.85[d]	0.036	1.0		
203	$2d_{3/2}$-$2d_{5/2}$	$\leq0.55\times10^{-9}$[b]	0.52[b]	≥1.4[b] 0.97[d]	0.008	0.08	236	8
215	$5/2$-$2d_{3/2}$	1.3×10^{-10}[c]	0.20[e]	1.25	0.028[f]	0.004	58	2
360	$5/2$-$1g_{7/2}$	3.7×10^{-11}[c]	-0.18[e]	0.14	0.014[f]	0.81	77	1
375	$3s_{1/2}$-$2d_{5/2}$			0.3[d]	0.06	0.56		
418	$5/2$-$2d_{5/2}$	5.5×10^{-12}[c]	-0.08[c]	0.13 0.1[d]	0.019[f]	0.07	18	0.2

a) Calculated using expressions given by KS and R. A. Sorensen, Phys. Rev. 133 (1964) B281 and the KS wave functions quoted by H. Langhoff, Nuclear Physics 63 (1965) 425

b) J. S. Geiger, Physics Letters 7 (1963) 48 (delayed coincidence, angular correlation and conversion electron measurements)

c) H. Langhoff, op. cit. (nuclear resonance fluorescence)

d) R. H. Davis, et al., Phys. Rev. 103 (1956) 1801 (Coulomb excitation)

e) Other values are allowed by the angular correlation results (see sec. 4.D.). The smaller values are assumed here on the basis of similar energy transitions in this and other isotopes.

f) The statistical factor has been set equal to 1.

5.A.i. Comparison of Electric Quadrupole Transition Rates

The reduced electric quadrupole transition probabilities are presented in Tables 7 and 8 as $B(E2)/(2j_f + 1)$, in units of $10^{-50}\ e^2\ cm^4$, for ease of comparison with theoretical predictions, in particular those of Sorenson.[58] These values are for the case of de-excitation of a state. The corresponding reduced transition rate for the population of a state by Coulomb excitation will be denoted $B(E2)_{ex}$. The two values are related by

$$B(E2;j \rightarrow j') = \frac{2j' + 1}{2j + 1} B(E2;\ j' \rightarrow j)_{ex} \quad .$$

The experimental B(E2) values are obtained from the paritial E2 mean-lives for gamma ray emission by use of the expression[58]

$$B(E2)_{exp} = 0.0825 \times 10^{-60} \times E_\gamma^{-5} \times T_\gamma^{-1}(E2)\ e^2\ cm^4$$

where E_γ is in MeV and $T_\gamma(E2)$ is the partial mean-life in seconds given by

$$T_\gamma(E2) = 1.44\epsilon^{-1}T_{1/2}(1 + \alpha_T)(1 + \frac{1}{\delta^2})$$

Here, ϵ is the branching ratio, $T_{1/2}$ is the measured half life of the nuclear state, α_T is the total conversion coefficient and δ^2 is the E2/M1 mixing ratio.

The experimental $B(E2)/(2j_f + 1)$ are compared with the single proton estimate given by[5]

$$\frac{B(E2)_{S.P.}}{2j_f+1} = \frac{\langle r^2 \rangle}{(2j_f+1)4\pi} [5(2j_f+1)(2\ell_f+1)\{W(\ell_f j_f \ell_i j_i; \tfrac{1}{2}\ 2) \times$$

$$(\ell_f 200|\ell_f 2 \ell_i 0)\}^2]e^2 \quad .$$

The quantity in square brackets is the "statistical factor," S,

which, for many cases,[59] can be approximated by S = 1. The quantities $W(\ell_f j_f \ell_i j_i; \frac{1}{2} 2)$ and $(\ell_f 200 | \ell_f 2 \ell_i 0)$ are Racah and Clebsch-Gordan coefficients, respectively. The expectation value of the square of the nuclear radius, $\langle r^2 \rangle$, is often[60] taken as $(3/5)R_o^2$ where $R_o = 1.2 \times 10^{-13} A^{1/3}$ cm is the "nuclear radius." This value has been used to calculate the single proton estimates given in column 6 of Tables 7 and 8.

The experimental B(E2) values, given in column 5, are, in every case, considerably larger than the single proton value. This result is not unique to these nuclei -- similar results having been obtained throughout the regions of spherical nuclei. (The same goes without saying for the deformed regions, where, as already mentioned, very large quadrupole effects are observed.) The B(E2) values for ^{121}Sb have also been calculated by Sorenson[58] using KS wave functions and the expression

$$\frac{B(E2)}{2j_f+1} = \left| C^{j_i}_{j_i 00} C^{j_f}_{j_f 00} e_{eff} \frac{\langle r^2 \rangle}{\sqrt{4\pi}} (-)^{j_f - \frac{1}{2}} (j_i j_f \tfrac{1}{2} - \tfrac{1}{2} | j_i j_f 20) \times \right.$$

$$(U_i U_f - V_i V_f) + \left(\frac{B(E2)_{0^+ \to 2^+}}{5} \right)^{1/2} \left[(-)^{j_i - j_f} (2j_f+1)^{-\frac{1}{2}} C^{j_f}_{j_f 00} C^{j_i}_{j_f 12} + \right.$$

$$\left. \left. (2j_i+1)^{-\frac{1}{2}} C^{j_f}_{j_i 12} C^{j_i}_{j_i 00} \right] \right|^2 .$$

The coefficients $C^{j'}_{jNR}$ are the contributions to the wave functions of the state j' of configurations consisting of quasiparticles of spin j coupled with N phonons with angular momentum R to the resultant j' . These eigenvectors are given by KS for a large number of states including several in ^{121}Sb and ^{127}I. The

quantities U and V are defined in such a way that U_i^2 gives the probability that the state (i) is unoccupied and V_i^2 has the opposite meaning. They are restricted by the relation $U_i^2 + V_i^2 = 1$. Methods for their calculation are given by KS. (They may also be determined experimentally, as has been done by Cohen and Price[61] for the Sn isotopes, using stripping and pickup reactions.) The B(E2) values obtained for ^{121}Sb, given in column 7 of Table 7, agree quite well with the experimental ones for the 469 and 572 keV pure E2 transitions. However, that obtained for the 506 keV transition is still an order of magnitude too small. The experimental value for the 68 keV transition is much larger than expected on the basis of values obtained for other transitions in this nucleus and may indicate that one or more of the data used in its calculation are in error. To bring this $B(E2)/(2j_f+1)$ into the range of other values (i.e., < 1) would require an increase by a factor of ≥ 20 in the partial mean-life of the 68 keV transition. The possibility that the mixing ratio of the 68 keV gammas determined in this study is in error was examined as follows: the mixing ratio required to give $B(E2)/(2j_f+1) < 1$ is $\delta < 0.04$. Using this value to calculate the angular correlation coefficient of the 68-506 keV cascade and employing data from other studies as discussed in Chap. 3.A., one obtains $A_2 \geq 0.17$ as compared to the experimental values $A_2 = 0.066 \pm 0.009$. This is well outside the error of our measurement. Thus, the suspected error is expected to exist elsewhere.

Similar comparisons with KS values of B(E2) were made in ^{127}I using Sorenson's expression, given above, and eigenvectors

for the ^{127}I states calculated by Sorensen and quoted by Langhoff.[53] The U's and V's were calculated using the expressions given by KS, except for the 418 keV state for which the values U = 1, V = 0 were assumed. The results are given in column 7 of Table 8. Only the values for the 145, 375 and 418 keV transitions are seen to be in reasonable agreement with experiment (within a factor of ~ 3). There appears to be a slight inconsistency in the data on the 203 keV level: the lifetime of the 203 keV level has been measured by Geiger[53] as $\leq 0.55 \times 10^{-9}$ sec, while the value deduced from the Coulomb excitation measurements of Davis, et al.,[61] (using the E2/M1 mixing ratio $\delta_{203} = +0.52$ obtained by Geiger[53]) is 0.75×10^{-9} sec. This result is reflected in the discrepancy in the B(E2) values for the 145 and 203 keV transitions. It is interesting that a similar disparity exists in ^{123}Te, as has been pointed out by Schmorak, et al.[62] The deviation in that case is in the same direction as found here, namely, the B(E2) obtained from Coulomb excitation cross section measurements is less than that from half life and mixing ratio measurements.

Quantitative data are also available for the 161 keV first excited state of ^{123}Sb from other studies. This state was not populated in the long-lived isomer of ^{123}Sn, when it decayed. Coulomb excitation cross section measurements by Fagg[43] give $B(E2)/(2j_f+1) = 0.04\ e^2 \times 10^{-50}\ cm^4$, which is $\sim 0.9 \times [B(E2)_{SP}/(2j_f+1)]$. The half life of this state was determined by Schmorak, et al.,[62] as 6.4×10^{-10} sec. The E2/M1 ratio has not yet been determined for the 161 keV transition so the two

measurements cannot be compared for compatibility.

5.A.ii. Comparison of M1 Transition Rates

It is also possible to compare experimental and theoretical values for the probability for emission of M1 radiation. The method used to make these comparisons is to present the ratio of the theoretical over the experimental reduced transition probabilities. The experimental values are obtained from the lifetimes of the nuclear states by use of the expression[63]

$$B(M1)_{exp} = \frac{1.43 \times 10^{-60}}{E^3(MeV) T_\gamma(M1)}$$

where $T_\gamma(M1)$ is the partial mean-life for M1 emission given by

$$T_\gamma(M1) = 1.44\epsilon^{-1} T_{1/2}(1 + \alpha_T)(1 + \delta^2) \quad .$$

In comparing the experimental result with the single proton estimate, it is found that the statistical factor for M1 emission is a rather cumbersome combination of 9-j and Racah coefficients. A reasonable estimate is given, however, by setting S = 1. This then yields the Weisskopf estimate.[64] The ratio of the Weisskopf estimate to the experimental value is given by

$$\frac{B(M1)_W}{B(M1)_{exp}} = \frac{E_\gamma^3 T_\gamma(M1)}{2.24 \times 10^{-14}} \text{ , where } E_\gamma \text{ is in MeV and } T_\gamma \text{ is in sec.}$$

These quantities, the M1 retardation factors, are given in column 8 of Tables 8 and 9. The experimental transition rates are from one to two orders of magnitude slower than the Weisskopf estimate. This is consistent with the M1 retardations found in other nuclei in this region of the isotope table.

The retardations of the M1 transitions in ^{127}I with respect to KS predictions have been calculated by Langhoff[53] and are given in column 9 of Table 9. Similar computations have been made for the ℓ-forbidden M1 transitions in ^{121}Sb by Sorensen[63] and these results are given in column 9 of Table 8. A similar retardation factor was obtained by Schmorak[62] for the 161 keV transition in ^{123}Sb. Using the half life quoted above, this gives a retardation of 140 over the single proton estimate. The corresponding value obtained by Sorensen is only ~ 3.

Although it has been pointed out by Geiger[53] that the KS predictions are not, in general, as good for M1 as for E2 transition rates, it appears that in these two nuclei, the agreement is rather good. In fact, all of the predicted values are within a factor of 10 of the corresponding experimental ones, which is better than for many of the theoretical E2 transition rates.

5.A.iii. Energy Level Systematics

In addition to predicting electromagnetic transition rates, as discussed above, any usable model should be able to give the spins, parities, and relative energies of the excited states of the nucleus. The low energy states of ^{121}Sb and ^{127}I are in qualitative agreement with predictions of several models. The single particle levels available to nucleons in the 50 to 82 shell, given in Chap. 1, are consistent with all of the observed low energy levels with the exception of the 418 keV $(5/2^+)$ state in ^{127}I. The KS calculations have been carried out only for the ground and first three excited states of ^{121}Sb. Since these three states are

essentially pure quasi-particle states, according to the KS calculations, the predicted spin sequence is essentially the same as for the single particle model. They do predict, however, the observed variation of the energies of the states with the addition of nucleon pairs. This variation is evident from the observed crossing of the $5/2^+$ and $7/2^+$ ground and first excited states between ^{121}Sb and ^{123}Sb. Similar computations have been made by Silverberg[65] for different values of the model parameters. The experimental variation of the energies of the $d_{5/2}$ and $g_{7/2}$ states in the odd-A antimony isotopes is shown in Figure 23, as is the corresponding trend in the iodine isotopes.

The KS calculations have been carried out for a much larger number of states in ^{127}I. The results are not too encouraging, however, since the first predicted spin 5/2 excited state lies considerably higher than is observed experimentally. Calculations have also been made using an intermediate coupling unified model in which the particle motion is coupled to collective vibrations of the nuclear core. This model has been applied to the study of ^{127}I and ^{129}I levels by Bannerjee and Gupta.[19] Although these calculations predict the approximate energies of a number of observed levels in $^{127,129}I$ it also predicts a preponderance of low-lying states which, as yet, have not been observed experimentally. One possible explanation of the poor agreement is that only the $2d_{5/2}$ and $1g_{7/2}$ single particle states were considered, with the remaining low energy states being treated as phonon-plus-particle states. It is believed that a more realistic interpretation of the observed levels, on the basis of this model, would be to

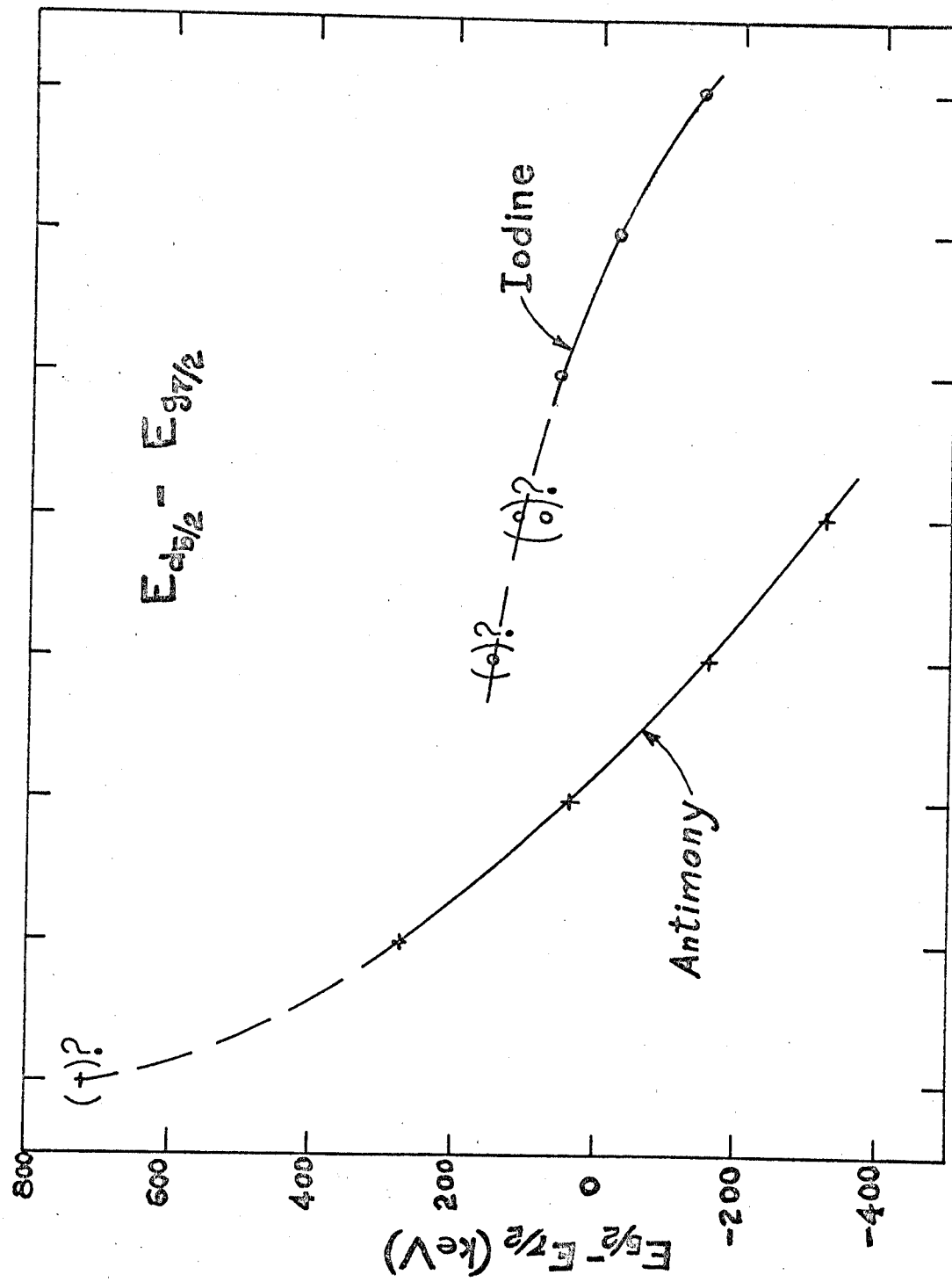

Figure 23. Energy systematics of the $2d_{5/2}$ and $1g_{7/2}$ states in odd-A antimony and iodine isotopes.

consider the ground and first three excited states as predominantly single particle states and treating those states at higher excitation energies as phonon-plus-particle states. This interpretation is based on the similarity between experimental observations and single particle predictions of the spins and parities of the ground and first three excited states of ^{127}I.

5.A.iv. Beta Transition Comparisons

It is also interesting to compare the allowed electron capture (^{121}Te) and beta (^{127}Te) transitions to the low-lying states in ^{121}Sb and ^{127}I, respectively. The log ft values for the transitions to the $1/2^+$ and $3/2^+$ states in ^{121}Sb and to the two $5/2^+$ states in ^{127}I are in the high end of the range usually considered for an allowed transition.[41] However, the transition to the 203 keV, $3/2^+$, state in ^{127}I is at least 3 orders of magnitude slower than expected (log ft $\sim$ 10.2). The same is true for the transitions to the $1/2^+$ state of ^{127}I at 375 keV which, within experimental error, is unpopulated in the decay of ^{127}Te. Both of these states are populated in the electron capture decay of the $3/2^+$ state of ^{127}Xe with transition probabilities well within the range for allowed transitions. The reason that these transitions are so unusually hindered is presently unknown.

5.B. The High Energy States

At higher excitation energies, very little information is available, making it impossible to make any quantitative comparisons with theoretical predictions. One can then only speculate as to the character of the nuclear states. In ^{121}Sb, ^{123}Sb and

^{127}I, the decay energy of the $11/2^-$ state of the parent is sufficient to populate only two or three of the multitude of high energy levels expected on the basis of comparisons with other nuclei in this region, for example, ^{119}Sb. Those which are populated in these three nuclei are found to be quite similar in that they all lie near the energy of the first excited state of the even-even nucleus corresponding to the core of the odd-A nucleus. These first excited states lie at 1180, 1140 and 665 keV in ^{120}Sn, ^{122}Sn and ^{126}Te, respectively. This result is in qualitative agreement with the level structure one would expect by coupling the low-lying single particle states to core excitations. The resultant "core-multiplet" should have its center of gravity near the energy of the excited state in the corresponding even-even nucleus, since the states should be only slightly perturbed by the interaction with the odd nucleon.[16]

One interesting feature of the higher energy states observed experimentally is that they all decay to the $7/2^+$ ground or first excited state. This fact may have a plausible explanation: if we assume the $11/2^-$ state of the parent nucleus is essentially a $1h_{11/2}$ single particle state, the beta or electron capture transitions to multiplets built on the $2d_{5/2}$ proton state would be expected to be ℓ-forbidden (i.e., $\Delta\ell = 3$), whereas, those to states formed from coupling the phonon to the $1g_{7/2}$ state would not be ℓ-forbidden. This assumes that the particle-core coupling is sufficiently weak that the particle character of the state is maintained and ℓ remains a good quantum number.

The same arguments can be applied to the levels in ^{125}Sb.

Here, sufficient energy is available in the beta decay of ^{125}Sn to populate states which may arise from coupling the particle motions to higher excitations of the core. The qualitative agreement with the core-coupling model is again obtained, with groups of levels being observed in the vicinity of excited states in ^{124}Sn. One possible interpretation of the observed ^{125}Sb levels is to consider those up to and including the 1419.8 keV state as due to coupling of the $1g_{7/2}$ particle state to the first excited state of the core, while those at higher energy can be considered as due to coupling to the second and higher excited states of the core. However, all of the observed states may not be explainable on the basis of core coupling: for example, the 1806.9, 2002.0, 2199.7 and 2276.0 keV states which decay primarily to the ground state. Such transitions would correspond, in the even-even nucleus, to transitions from the second or higher excited state to the ground state, which are usually observed to be weaker than transitions to the first excited state.[66] Such states may therefore be due to some other type of excitation whose character can only be decided when more quantitative data on these levels become available.

One is also tempted to interpret the 1419.8 and 1890.6 keV levels as members of core multiplets on the basis of the E2/M1 mixing ratios for the 469.6 and 1890.6 keV transitions. These were found to be $\geq 10^3$ times the Weisskopf estimate, in keeping with the expected enhancement of the E2 transition rates from the second to the first multiplet and from the first multiplet to the ground state. This result appears to lose some of its

significance, however, when it is found that a similar enhancement is obtained for the 331.9 keV transition, which, in the present interpretation, is assumed to be between two states of the same multiplet. Such transitions, according to de-Shalit,[16] are expected to proceed predominantly by emission of M1 radiation.

One disconcerting fact, which tends to cast some doubt on the present interpretation of the high energy levels in ^{121}Sb and ^{123}Sb as core-multiplets is that, as far as can be determined, they have not been excited in Coulomb excitation studies.[43] For a multiplet built on the first 2^+ excited state of the even core, we should have[16]

$$\sum_J B(E2;J_g \rightarrow J) = B(E2;0^+ \rightarrow 2^+)$$

That is, the sum of the reduced transition probabilities from the ground state, J_g, of the odd-A nucleus to the multiplet states, J, is just equal to that for exciting the 2^+ state in the even core nucleus. The probability for exciting a given J state can then be written as

$$B(E2;J_g \rightarrow J) = \frac{2J+1}{5(2J_g+1)} B(E2;\ 0^+ \rightarrow 2^+)$$

The values of $B(E2;\ 0^+ \rightarrow 2^+)$ are found to be relatively large; for example, $\sim 20 \times 10^{-50}\ e^2\ cm^4$ and $\sim 40\text{-}65 \times 10^{-50}\ e^2\ cm^4$ for the even tin and tellurium isotopes, respectively. Thus, at least the high spin multiplet states should be strongly excited. This assumes, of course, identical experimental conditions for both the odd-A and the even isotope cases. The cross section for E2 Coulomb excitation, as given by Alder, et al.,[66] is

$$\sigma_{E2} = \left(\frac{m_o v}{\hbar Ze}\right)^2 \times B(E2)_{ex} \times f_{E2}$$

where the function f_{E2} decreases rapidly with decreasing energy of the incident ions. In the cases being considered here, that is, ^{121}Sb and ^{123}Sb, the earlier studies by Fagg were made with $\sim$ 5.2 MeV alpha particles, while $\sim$ 10 MeV alphas were used in the measurements on the corresponding tin isotopes.[67] Using the f_{E2} curves given by Alder, et al., this change in energy by a factor of ~ 2 is found to result in a change by a factor of $\sim$10 for f_{E2}. It may be, therefore, that the non-observation of the higher excited states in these earlier works was due to the reduction in the cross section by the decrease in f_{E2} rather than to a decrease in B(E2). No conclusions can be drawn on the later report by Robinson, et al., using 7-9 MeV alphas, since no spectra are presented and no indication given of whether high energy transitions were sought. The need for additional information on the higher energy regions of the level spectrum of these antimony isotopes is clearly indicated.

In contrast, levels in ^{127}I at 630 and 750 keV have reportedly[52] been excited by Coulomb excitation using $\sim$3 MeV protons. The relatively large values $B(E2)_{ex} = 10 \times 10^{-50}$ e^2 cm^4 are found for both states. These can be compared with the $B(E2)_{ex}$ for exciting the first 2^+ state in ^{126}Te which is $\sim 40 \times 10^{-50}$ e^2 cm^4. These states could therefore constitute part of a multiplet built on the $5/2^+$ ground state of ^{127}I.

BIBLIOGRAPHY

(1) Nuclear Data Sheets (The National Academy of Sciences - National Research Council, Washington, D. C.)

(2) Nuclear Theory Index (NAS-NRC, Washington, D. C.)

(3) Nuclear Science Abstracts (USAEC, Division of Technical Information)

Physics Abstracts (The Institution of Electrical Engineers, London)

(4) M. G. Mayer and J. H. D. Jensen, Elementary Theory of Nuclear Shell Structure (John Wiley and Sons, Inc., New York, 1955)

(5) M. A. Preston, Physics of the Nucleus (Addison-Wesley Publishing Co., Inc., Reading, Mass., 1962) Chap. 7

(6) Amos de-Shalit and Igal Talmi, Nuclear Shell Theory (Academic Press, New York, 1963)

(7) M. A. Preston, loc. cit., Chap. 4

D. M. Brink, Collective Motion in Nuclei in Progress in Nuclear Physics, vol. 8 (Pergamon Press Inc., New York, 1960) pg. 99

(8) S. G. Nilsson, Mat. Fys. Med. Dan. Vid. Selsk. 29, No. 16 (1955)

(9) E. Marshalek, L. W. Person and R. K. Sheline, Revs. Mod. Phys. 35 (1963) 108

(10) D. Bes and Z. Szymanski, Nuclear Physics 28 (1961) 41

(11) Z. Szymanski, Nuclear Physics 28 (1961) 63

(12) A. Bohr, Mat. Fys. Medd. Dan. Vid. Selsk. 26, No. 14 (1952)

(13) A. S. Davydov and G. F. Filipov, Nuclear Physics 8 (1958) 237

(14) A. K. Kerman, Mat. Fys. Medd. Dan. Vid. Selsk. 30, No. 15 (1956)

(15) V. V. Pashkevich and R. A. Sardaryan, Nuclear Physics 65 (1965) 401

(16) A. de-Shalit, Phys. Rev. 122 (1961) 1530

(17) D. C. Choudhury, Mat. Fys. Medd. Dan. Vid. Selsk. 28, No. 4 (1954)

(18) N. K. Glendenning, Phys. Rev. 119 (1960) 213

(19) B. Bannerjee and K. K. Gupta, Nuclear Physics 30 (1962) 227

(20) S. T. Belyaev, Mat. Fys. Medd. Dan. Vid. Selsk. 31, No. 11 (1959)

(21) L. S. Kisslinger and R. A. Sorensen, Revs. Mod. Phys. 35 (1963) 853

(22) Nuclear Data Sheets, NRC 60-6-63

(23) R. W. Fink, G. Andersson and J. Kantele, Ark. Fys. 19 (1961) 323

(24) A. S. Newton and W. L. McDonell in The Radiochemistry of Tin, by W. E. Nervik (National Academy of Sciences NAS-NS 3023)

(25) R. L. Heath, IDO-16880-1 (Aug. 1964)

(26) M. J. L. Yates in α- β -γ Ray Spectroscopy, edited by Kai Siegbahn (North-Holland Publishing Co., Amsterdam, 1965) Appendix 9

(27) J. H. Neiler and P. R. Bell, in α- β -γ Ray Spectroscopy, loc. cit., chap. 5

(28) W. M. Gibson, G. L. Miller and P. F. Donovan, in α- β -γ Ray Spectroscopy, loc. cit., chap. 6

(29) Nuclear Data Sheets, NRC 60-5-27

(30) R. van Lieshout, A. H. Wapstra, R. A. Ricci and R. K. Girgis, in α- β -γ Ray Spectroscopy, loc. cit., chap. 8

(31) R. L. Auble, A Survey of Angular Correlation Theory with an Application to ^{121}Te, MS Thesis (1962)

(32) Nuclear Data Sheets, NRC 61-2-134

(33) Nuclear Data Sheets, NRC 60-4-74, 75, 80, 81

(34) S. Monaro, O. Kistner and A. C. Li, Bull. Am. Phys. Soc. 8, No. 4 (1963) 532, J10

(35) R. E. Snyder and G. B. Beard, Phys. Lett. 15 (1965) 264 and Private Communication

(36) R. K. Gupta, Nuovo Cim. 17 (1960) 665
R. Bhattacharyya and S. Shastry, Nuclear Physics 41 (1963) 184

(37) F. R. Metzger and H. Langhoff, Phys. Rev. 132 (1963) 1753

(38) Y. Y. Chu, O. C. Kistner, A. C. Li, S. Monaro and M. L. Perlman, Phys. Rev. 133 (1964) B1361

(39) R. Bhattacharyya and S. Shastry, op. cit.

(40) M. E. Rose, Internal Conversion Coefficients (North-Holland Publishing Co., Amsterdam, 1958)

(40a) L. A. Sliv and I. M. Band, Coefficients of Internal Conversion of Gamma Radiation (U.S.S.R. Academy of Sciences, Moscow-Leningrad, 1956, 1958); also Reports 57 ICC K1 and 58 ICC L1 (Physics Dept., Univ. of Illinois, Urbana, 1957, 1958)

(41) The use of the quantities, ft, to compare β decay rates is discussed, for example, by:

E. J. Konopinski and M. E. Rose, The Theory of Nuclear Decay in α-β-γ Ray Spectroscopy, loc. cit., Chap. 23

A nomogram from which the value of log ft can be immediately

determined for a given end point energy and lifetime, is given by:

A. H. Wapstra, G. J. Nijgh and R. Van Lieshout, Nuclear Spectroscopy Tables (North-Holland Publishing Co., Amsterdam, 1959)

A comparison of the experimental values is given by:

C. E. Gleit, Chung-Wai Tang and C. D. Coryell, Beta Decay Transition Probabilities, Nuclear Data Tables (National Research Council)

(42) Nuclear Data Sheets, NRC 60-2-99, 105, 106

(43) L. W. Fagg, Phys. Rev. 109 (1958) 100

R. L. Robinson, P. H. Stelson, F. K. McGowan, J. L. C. Ford, Jr., W. T. Milner, ORNL-3778 (1964) pg. 116

(44) J. P. Palmer and L. J. Laslett, AECU-1220 (1951)

(45) A. C. G. Mitchell, Procedures for the Investigation of Disintegration Schemes, in α- β-γ Ray Spectroscopy, loc. cit., pg. 488

(46) Nuclear Data Sheets, NRC 60-6-63, 68

(47) Nuclear Data Sheets, NRC 60-6-91

S. H. Devare and H. G. Devare, Phys. Rev. 133 (1964) B568

(48) G. T. Ewan and A. J. Tavendale, A. E. C. L. No. 2079 (1964)

(49) Nuclear Data Sheets, 5-6-38, 39 (Apr. 1964)

(50) S. H. Devare and H. G. Devare, Preprint (1965)

(51) S. Ofer, Phys. Rev. 114 (1959) 870

(52) Nuclear Data Sheets, NRC 61-1-72, 76

(53) J. S. Geiger, Phys. Lett. 7 (1963) 48
J. S. Geiger, R. L. Graham, I. Bergstrom and F. Brown, Nuclear Physics, to be published

(54) A. Abragam and R. V. Pound, Phys. Rev. 92 (1953) 943
H. Frauenfelder and R. M. Steffen, Angular Distribution of Nuclear Radiation, in α-β-γ Ray Spectroscopy, loc. cit., chap. 19

(55) G. J. Perlow and S. L. Ruby, Phys. Lett. 13 (1964) 198

(56) W. B. Chaffee, private communication

(57) A. H. Wapstra, G. J. Nijgh and R. Van Lieshout, loc. cit., pg. 114

(58) R. A. Sorensen, Phys. Rev. 133 (1964) B281

(59) Amos de-Shalit and Igal Jalmi, loc. cit., pg. 167

(60) A. H. Wapstra, G. J. Nijgh and R. Van Lieshout, loc. cit., pg. 116
M. A. Preston, loc. cit., pg. 46

(61) R. H. Davis, A. S. Divatia, D. A. Lind and R. D. Moffat, Phys. Rev. 103 (1956) 1801

(62) M. Schmorak, A. C. Li and A. Schwarzschild, Phys. Rev. 130 (1963) 727

(63) R. A. Sorensen, Phys. Rev. 132 (1963) 2270

(64) M. A. Preston, loc. cit., pg. 335

A. H. Wapstra, G. J. Nijgh and R. Van Lieshout, loc. cit., pg. 71

(65) Lars Silverberg, Ark. Fys. 20 (1961) 341

(66) K. Alder, A. Bohr, T. Huus, B. Mottelson and A. Winther, Rev. Mod. Phys. 28 (1956) 432

(67) P. H. Stelson and F. K. McGowan, Phys. Rev. 110 (1958) 489